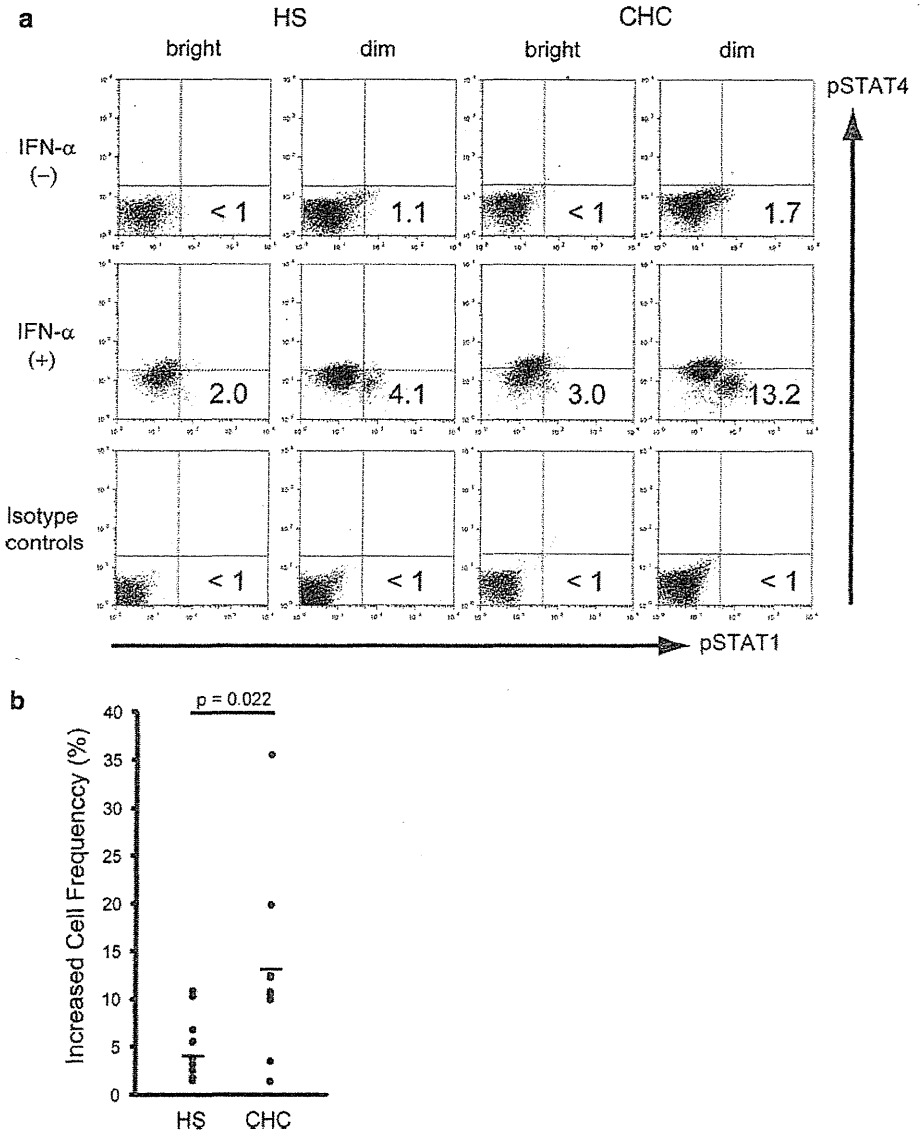

Fig. 5 Relationship between STAT1/4 phosphorylation occurring in response to IFN-α in NK cell subsets. pSTAT1 and pSTAT4 protein levels were simultaneously evaluated by flow cytometry with isotype control staining. PBMCs were derived from patients with chronic HCV infection (CHC) ($n = 9$) and healthy subjects (HS) ($n = 11$). Prepared PBMCs were unstimulated or stimulated with natural IFN-α for 90 min in vitro, and then collected. pSTAT1 and pSTAT4 protein levels in $CD56^{bright}$ NK (bright) and $CD56^{dim}$ NK (dim) cell subsets were evaluated by flow cytometry, electronically gating on CD56 bright $CD3^-$ cells and CD56 dim $CD3^-$ cells. **a** Representative dot plots of untreated or IFN-α treated cells stained with antibody or isotype controls from a patient and a healthy subject (*HS*) are shown. *Numbers* are frequencies of gated cells that strongly phosphorylated STAT1 but weakly phosphorylated STAT4 in the corresponding subsets. **b** Increased cell frequency was determined by subtracting the gated cell frequency of unstimulated cells from those of stimulated cells. Comparisons of the increased cell frequency of the high-pSTAT1 population in response to IFN-α stimulation in the $CD56^{dim}$ NK cell subset between CHC and HS are shown with the statistically significant p value. Each *circle* represents individual data. *Horizontal bars* represent means. Statistical significance was analyzed using the unpaired Student's t-test

STAT1 signaling pathway being less activated in CHB than in CHC [34].

Lines of evidence have shown that $CD56^{dim}$ NK cells, but not $CD56^{bright}$ NK cells, decrease in number in peripheral blood in patients with CHC [12, 14, 15, 35]. In agreement with these reports, we observed a lower frequency of $CD56^{dim}$ NK cells, but not of $CD56^{bright}$ NK cells, in the CHC patients than in the HS (Fig. 1b). Although we observed significant up-regulation of STAT1 expression in both $CD56^{bright}$ NK cells and $CD56^{dim}$ NK cells, the magnitude of the up-regulation of STAT1 expression in the CHC patients, compared with that in the

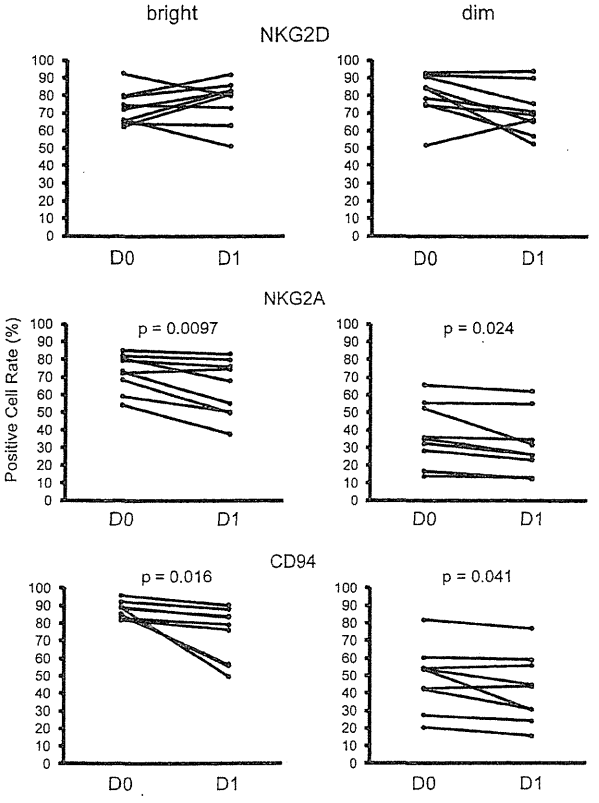

Fig. 6 Regulation of NK receptor expression in response to IFN-α-based therapy. The expression of NK activating or inhibitory receptors, NKG2D or NKG2A and CD94, respectively, on $CD56^{bright}$ NK (bright) and $CD56^{dim}$ NK (dim) cell subsets was evaluated by flow cytometry with isotype control staining, electronically gating on CD56 bright $CD3^-$ cells and CD56 dim $CD3^-$ cells. PBMCs were derived from patients treated with IFN-α-based therapy ($n = 9$) before (*D0*) and 1 day after (*D1*) the initiation of the therapy. Positive cells (positive cell rate) were determined based on isotype control staining. The changes in the NK receptor expression levels between D0 and D1 are shown as positive cell rates with the statistically significant p values. Each *circle* represents individual data. Statistical significance was analyzed using the paired Student's t-test

HS, was clearly greater in $CD56^{dim}$ NK cells than in $CD56^{bright}$ NK cells (Fig. 3b). Considering that STAT1 transmits the anti-proliferative effects induced by IFN-α [36–38], the greater up-regulation of STAT1 in $CD56^{dim}$ NK cells, compared with that of $CD56^{bright}$ NK cells, might have resulted in the significantly reduced frequency in $CD56^{dim}$ NK cells but not in $CD56^{bright}$ NK cells. Further study is required to examine this.

The most prolific producer of IFN-γ is the $CD56^{bright}$ NK cell rather than the $CD56^{dim}$ NK cell [4, 5]. In the present study, we found that $CD56^{bright}$ NK cells responded to IL-12 to phosphorylate STAT4 much more than $CD56^{dim}$ NK cells (Fig. 4a, b). IL-12 is one of the strongest stimulators of IFN-γ production from NK cells, which is transmitted by STAT4 phosphorylation [1, 3, 39, 40]. The preferential activation of STAT4 in $CD56^{bright}$ NK cells, compared with $CD56^{dim}$ NK cells, might be one of the underlying mechanisms by which $CD56^{bright}$ NK cells, compared with $CD56^{dim}$ NK cells, are armed to produce IFN-γ. On the other hand, we found that $CD56^{dim}$ NK cells responded to IFN-γ to phosphorylate STAT1, while $CD56^{bright}$ NK cells hardly did so (Fig. 4a, b). Moreover, some of the $CD56^{dim}$ NK cells responded to IFN-α to more strongly phosphorylate STAT1 than $CD56^{bright}$ NK cells (Fig. 5a). The $CD56^{dim}$ NK cells are strongly cytolytic armed effector cells [4, 5]. IFN-α or IFN-γ is one of the strongest inducers of the cytolytic function of NK cells, which is transmitted by STAT1 phosphorylation [1, 3, 38, 41]. Thus, the predominant activation of STAT1 in $CD56^{dim}$ NK cells, compared with $CD56^{bright}$ NK cells, might be one of the underlying mechanisms by which $CD56^{dim}$ NK cells become armed with a strong cytotoxic function. The differences in cytokine response to activate STAT molecules between these NK cell subsets might lead to the differences in their armed functions, such as cytolysis and cytokine production.

Ahlenstiel et al. [42] have recently reported that chronic exposure to HCV-induced IFN-α rendered NK cells with a functional polarization toward a cytotoxic phenotype, but without an increase in IFN-γ production. Moreover, Oliviero et al. [16] showed that NK cells from CHC patients were of a predominantly activating phenotype and that these phenotypic changes were associated with enhanced cytotoxic activity and defective IFN-γ production. These reports may be associated with our finding that NK cells, including $CD56^{bright}$ and $CD56^{dim}$ subsets, from the CHC patients displayed a high level of STAT1 expression (Fig. 3). Cytotoxic molecules such as perforin and granzyme, as well as STAT1, are among the ISGs [28, 41]. A high level of STAT1 in NK cells, particularly in $CD56^{dim}$ NK cells that are armed with a cytolytic function, in CHC patients might correspond to a high level of cytotoxic molecules in NK cells, resulting in enhanced cytotoxic activity. Indeed, the frequency of the population that strongly phosphorylated STAT1 upon IFN-α stimulation in $CD56^{dim}$ NK cells was significantly higher in the CHC patients than in the HS (Fig. 5b). This population might be highly armed cells with a cytolytic function. On the other hand, it has been reported that the STAT1 expression level in NK cells was correlated negatively with the activation of STAT4 to produce IFN-γ in response to IFN-α in NK cells [22, 24]. A high level of STAT1 in NK cells, particularly in $CD56^{bright}$ NK cells that are armed to produce IFN-γ, might cause defective IFN-γ production in the NK cells of patients with CHC.

Recent studies have demonstrated that a higher level of ISGs in hepatocytes as well as in PBMCs before IFN-α-based therapy is associated with resistance to this therapy

[32, 43]. We have also reported that a small number of CHC patients treated with IFN-α-based therapy revealed a tendency, in those who had a higher level of STAT1 (which is one of the ISGs) in the total NK cell population, to not respond well to the therapy in the early phase, such as in week 8 after its initiation [24]. In the present study, we did not observe a significant correlation between the STAT1 expression level in the NK cell subsets and the sensitivity to IFN-α based therapy, but we did find a tendency of those who had a higher level of STAT1 in the NK cell subsets to not respond well to the therapy in the early phase, such as in week 8 after its initiation (T. Miyagi et al. unpublished data). The number of evaluated patients, however, was small. More data on treated patients will be required to accurately evaluate the relationship between the STAT1 expression level in the NK cell subsets and the therapy outcome.

We have recently reported that NKG2D expression on NK cells could be down-regulated by the soluble major histocompatibility complex class I-related chain A (MICA), which was increased in patients with CHC compared with healthy controls [44]. In the present study, NKG2D expression levels on both $CD56^{bright}$ NK cells and $CD56^{dim}$ NK cells from the CHC patients were significantly lower than those from the HS (Fig. 2). Thus, the lower NKG2D expression on either $CD56^{bright}$ NK cells or $CD56^{dim}$ NK cells in patients with CHC might be caused by the increased soluble MICA. In response to IFN-α treatment in vivo, the expression of NKG2A/CD94 was down-regulated in both subsets in the CHC patients. In vitro stimulation of NK cells with IFN-α did not down-regulate or up-regulate the messenger RNA expression of NKG2A/CD94 in NK cells (T. Miyagi et al. unpublished data). Thus, the lower expression of NKG2A/CD94 might be modulated not directly but indirectly by in vivo IFN-α treatment.

In the present study, we investigated how the NK cell subsets differed in frequency, phenotype, and cytokine response, and also how chronic HCV infection modified these differences. $CD56^{bright}$ NK cells had a relatively higher level of intracellular STAT1 expression than $CD56^{dim}$ NK cells in the HS. Both $CD56^{bright}$ NK cells and $CD56^{dim}$ NK cells from the CHC patients displayed remarkably higher levels of STAT1 expression than those from the HS, without any significant differences between these subsets. Upon in vitro stimulation with cytokines such as IL-12, IFN-γ, and IFN-α, $CD56^{bright}$ NK cells and $CD56^{dim}$ NK cells phosphorylated STAT1/4 differently. These differences between the NK cell subsets in frequency, phenotype, and cytokine response were partly altered in the CHC patients, suggesting their possible association with the persistence of HCV infection and the resistance to IFN-α based therapy. These observations suggest the possibility of cellular or molecular targets for the treatment of chronic HCV infection.

Acknowledgments This work was supported by Grants-in-aid for Scientific Research (to T. Takehara and T. Miyagi) and by a grant for the Global Centers of Excellence Program (to T. Miyagi) from the Ministry of Education, Culture, Sports, Science and Technology of Japan and a Grant-in-aid (to T. Takehara) from the Ministry of Health, Labour and Welfare of Japan.

References

1. Biron CA, Nguyen KB, Pien GC, Cousens LP, Salazar-Mather TP. Natural killer cells in antiviral defense: function and regulation by innate cytokines. Annu Rev Immunol. 1999;17:189–220.
2. Farrar MA, Schreiber RD. The molecular cell biology of interferon-gamma and its receptor. Annu Rev Immunol. 1993;11:571–611.
3. Lee SH, Miyagi T, Biron CA. Keeping NK cells in highly regulated antiviral warfare. Trends Immunol. 2007;28:252–9.
4. Cooper MA, Fehniger TA, Caligiuri MA. The biology of human natural killer-cell subsets. Trends Immunol. 2001;22:633–40.
5. Caligiuri MA. Human natural killer cells. Blood. 2008;112:461–9.
6. Liang TJ, Rehermann B, Seeff LB, Hoofnagle JH. Pathogenesis, natural history, treatment, and prevention of hepatitis C. Ann Intern Med. 2000;132:296–305.
7. Kamal SM, Fouly AE, Kamel RR, Hockenjos B, Al Tawil A, Khalifa KE, et al. Peginterferon alfa-2b therapy in acute hepatitis C: impact of onset of therapy on sustained virologic response. Gastroenterology. 2006;130:632–8.
8. Manns MP, McHutchison JG, Gordon SC, Rustgi VK, Shiffman M, Reindollar R, et al. Peginterferon alfa-2b plus ribavirin compared with interferon alfa-2b plus ribavirin for initial treatment of chronic hepatitis C: a randomised trial. Lancet. 2001;358:958–65.
9. Fried MW, Shiffman ML, Reddy KR, Smith C, Marinos G, Gonçales FL Jr, et al. Peginterferon alfa-2a plus ribavirin for chronic hepatitis C virus infection. N Engl J Med. 2002;347:975–82.
10. Santantonio T, Fasano M, Sinisi E, Guastadisegni A, Casalino C, Mazzola M, et al. Efficacy of a 24-week course of PEG-interferon alpha-2b monotherapy in patients with acute hepatitis C after failure of spontaneous clearance. J Hepatol. 2005;42:329–33.
11. Meier UC, Owen RE, Taylor E, Worth A, Naoumov N, Willberg C, et al. Shared alterations in NK cell frequency, phenotype, and function in chronic human immunodeficiency virus and hepatitis C virus infections. J Virol. 2005;79:12365–74.
12. Morishima C, Paschal DM, Wang CC, Yoshihara CS, Wood BL, Yeo AE, et al. Decreased NK cell frequency in chronic hepatitis C does not affect ex vivo cytolytic killing. Hepatology. 2006;43:573–80.
13. Nattermann J, Feldmann G, Ahlenstiel G, Langhans B, Sauerbruch T, Spengler U. Surface expression and cytolytic function of natural killer cell receptors is altered in chronic hepatitis C. Gut. 2006;55:869–77.
14. Golden-Mason L, Madrigal-Estebas L, McGrath E, Conroy MJ, Ryan EJ, Hegarty JE, et al. Altered natural killer cell subset distributions in resolved and persistent hepatitis C virus infection following single source exposure. Gut. 2008;57:1121–8.
15. Bonorino P, Ramzan M, Camous X, Dufeu-Duchesne T, Thélu MA, Sturm N, et al. Fine characterization of intrahepatic NK cells

expressing natural killer receptors in chronic hepatitis B and C. J Hepatol. 2009;51:458–67.
16. Oliviero B, Varchetta S, Paudice E, Michelone G, Zaramella M, Mavilio D, et al. Natural killer cell functional dichotomy in chronic hepatitis B and chronic hepatitis C virus infections. Gastroenterology. 2009;137:1151–60, 1160.e1–7.
17. Takehara T, Hayashi N. Natural killer cells in hepatitis C virus infection: from innate immunity to adaptive immunity. Clin Gastroenterol Hepatol. 2005;3:S78–81.
18. Golden-Mason L, Rosen HR. Natural killer cells: primary target for hepatitis C virus immune evasion strategies? Liver Transpl. 2006;12:363–72.
19. Szabo G, Chang S, Dolganiuc A. Altered innate immunity in chronic hepatitis C infection: cause or effect? Hepatology. 2007;46:1279–90.
20. Bedossa P, Poynard T. An algorithm for the grading of activity in chronic hepatitis C. The METAVIR Cooperative Study Group. Hepatology. 1996;24:289–93.
21. Jinushi M, Takehara T, Tatsumi T, Kanto T, Miyagi T, Suzuki T, et al. Negative regulation of NK cell activities by inhibitory receptor CD94/NKG2A leads to altered NK cell-induced modulation of dendritic cell functions in chronic hepatitis C virus infection. J Immunol. 2004;173:6072–81.
22. Miyagi T, Gil MP, Wang X, Louten J, Chu WM, Biron CA. High basal STAT4 balanced by STAT1 induction to control type 1 interferon effects in natural killer cells. J Exp Med. 2007;204:2383–96.
23. Miyagi T, Lee SH, Biron CA. Intracellular staining for analysis of the expression and phosphorylation of signal transducers and activators of transcription (STATs) in NK cells. Methods Mol Biol. 2010;612:159–75.
24. Miyagi T, Takehara T, Nishio K, Shimizu S, Kohga K, Li W, et al. Altered interferon-alpha-signaling in natural killer cells from patients with chronic hepatitis C virus infection. J Hepatol. 2010;53:424–30.
25. Uzel G, Frucht DM, Fleisher TA, Holland SM. Detection of intracellular phosphorylated STAT-4 by flow cytometry. Clin Immunol. 2001;100:270–6.
26. Krutzik PO, Clutter MR, Nolan GP. Coordinate analysis of murine immune cell surface markers and intracellular phosphoproteins by flow cytometry. J Immunol. 2005;175:2357–65.
27. Der SD, Zhou A, Williams BR, Silverman RH. Identification of genes differentially regulated by interferon alpha, beta, or gamma using oligonucleotide arrays. Proc Natl Acad Sci USA. 1998;95:15623–8.
28. Ji X, Cheung R, Cooper S, Li Q, Greenberg HB, He XS. Interferon alfa regulated gene expression in patients initiating interferon treatment for chronic hepatitis C. Hepatology. 2003;37:610–21.
29. Pfeffer LM, Madey MA, Riely CA, Fleckenstein JF. The induction of type I interferon production in hepatitis C-infected patients. J Interferon Cytokine Res. 2009;29:299–306.
30. Dolganiuc A, Norkina O, Kodys K, Catalano D, Bakis G, Marshall C, et al. Viral and host factors induce macrophage activation and loss of toll-like receptor tolerance in chronic HCV infection. Gastroenterology. 2007;133:1627–36.
31. Chen L, Borozan I, Sun J, Guindi M, Fischer S, Feld J, et al. Cell-type specific gene expression signature in liver underlies response to interferon therapy in chronic hepatitis C infection. Gastroenterology. 2010;138:1123–33.
32. Sarasin-Filipowicz M, Oakeley EJ, Duong FH, Christen V, Terracciano L, Filipowicz W, et al. Interferon signaling and treatment outcome in chronic hepatitis C. Proc Natl Acad Sci USA. 2008;105:7034–9.
33. Tateno M, Honda M, Kawamura T, Honda H, Kaneko S. Expression profiling of peripheral-blood mononuclear cells from patients with chronic hepatitis C undergoing interferon therapy. J Infect Dis. 2007;195:255–67.
34. Honda M, Yamashita T, Ueda T, Takatori H, Nishino R, Kaneko S. Different signaling pathways in the livers of patients with chronic hepatitis B or chronic hepatitis C. Hepatology. 2006;44:1122–38.
35. Amadei B, Urbani S, Cazaly A, Fisicaro P, Zerbini A, Ahmed P, et al. Activation of natural killer cells during acute infection with hepatitis C virus. Gastroenterology. 2010;138:1536–45.
36. Bromberg JF, Horvath CM, Wen Z, Schreiber RD, Darnell JE Jr. Transcriptionally active Stat1 is required for the antiproliferative effects of both interferon alpha and interferon gamma. Proc Natl Acad Sci USA. 1996;93:7673–8.
37. Tanabe Y, Nishibori T, Su L, Arduini RM, Baker DP, David M. Cutting edge: role of STAT1, STAT3, and STAT5 in IFN-alpha beta responses in T lymphocytes. J Immunol. 2005;174:609–13.
38. García-Sastre A, Biron CA. Type 1 interferons and the virus–host relationship: a lesson in détente. Science. 2006;312:879–82.
39. Cho SS, Bacon CM, Sudarshan C, Rees RC, Finbloom D, Pine R, et al. Activation of STAT4 by IL-12 and IFN-alpha: evidence for the involvement of ligand-induced tyrosine and serine phosphorylation. J Immunol. 1996;157:4781–9.
40. Matikainen S, Paananen A, Miettinen M, Kurimoto M, Timonen T, Julkunen I, et al. IFN-alpha and IL-18 synergistically enhance IFN-gamma production in human NK cells: differential regulation of Stat4 activation and IFN-gamma gene expression by IFN-alpha and IL-12. Eur J Immunol. 2001;31:2236–45.
41. Liang S, Wei H, Sun R, Tian Z. IFN alpha regulates NK cell cytotoxicity through STAT1 pathway. Cytokine. 2003;23:190–9.
42. Ahlenstiel G, Titerence RH, Koh C, Edlich B, Feld JJ, Rotman Y, et al. Natural killer cells are polarized toward cytotoxicity in chronic hepatitis C in an interferon-alfa-dependent manner. Gastroenterology. 2010;138:325–35.
43. Feld JJ, Nanda S, Huang Y, Chen W, Cam M, Pusek SN, et al. Hepatic gene expression during treatment with peginterferon and ribavirin: identifying molecular pathways for treatment response. Hepatology. 2007;46:1548–63.
44. Kohga K, Takehara T, Tatsumi T, Ohkawa K, Miyagi T, Hiramatsu N, et al. Serum levels of soluble major histocompatibility complex (MHC) class I-related chain A in patients with chronic liver diseases and changes during transcatheter arterial embolization for hepatocellular carcinoma. Cancer Sci. 2008;99:1643–9.

J Gastroenterol (2011) 46:1031–1037
DOI 10.1007/s00535-011-0409-7

ORIGINAL ARTICLE—LIVER, PANCREAS, AND BILIARY TRACT

Efficacy of re-treatment with pegylated interferon plus ribavirin combination therapy for patients with chronic hepatitis C in Japan

Tsugiko Oze · Naoki Hiramatsu · Takayuki Yakushijin · Kiyoshi Mochizuki · Masahide Oshita · Hideki Hagiwara · Eiji Mita · Toshifumi Ito · Yoshiaki Inui · Hiroyuki Fukui · Taizo Hijioka · Kazuhiro Katayama · Shinji Tamura · Harumasa Yoshihara · Atsuo Inoue · Yasuharu Imai · Eijiro Hayashi · Michio Kato · Atsushi Hosui · Takuya Miyagi · Hisashi Ishida · Yuichi Yoshida · Tomohide Tatsumi · Shinichi Kiso · Tatsuya Kanto · Akinori Kasahara · Tetsuo Takehara · Norio Hayashi

Received: 27 December 2010 / Accepted: 31 March 2011 / Published online: 3 May 2011

Abstract
Background It is still not known which patients with chronic hepatitis C who failed to respond to previous pegylated interferon (Peg-IFN) plus ribavirin therapy can benefit from re-treatment.
Methods Seventy-four patients (HCV genotype 1, $n = 56$, genotype 2, $n = 18$) were re-treated with Peg-IFN plus ribavirin.
Results On re-treatment, the sustained virologic response (SVR) rate was 41% for genotype 1 and 56% for genotype 2. With genotype 1, the factors associated with an SVR were previous treatment response and the serum hepatitis C virus (HCV) RNA level at the start of re-treatment. Patients with a $\geq$2-log decrease in HCV RNA at week 12 (partial early virologic response, p-EVR) in previous treatment had significantly higher SVR rates than those without these

T. Oze · N. Hiramatsu (✉) · T. Yakushijin · K. Mochizuki · A. Hosui · T. Miyagi · H. Ishida · Y. Yoshida · T. Tatsumi · S. Kiso · T. Kanto · A. Kasahara · T. Takehara
Department of Gastroenterology and Hepatology, Osaka University Graduate School of Medicine, 2-2, Yamadaoka, Suita, Osaka 565-0871, Japan
e-mail: hiramatsu@gh.med.osaka-u.ac.jp

M. Oshita
Osaka Police Hospital, Osaka, Japan

H. Hagiwara · N. Hayashi
Kansai Rousai Hospital, Amagasaki, Japan

E. Mita
National Hospital Organization Osaka National Hospital, Osaka, Japan

T. Ito
Osaka Koseinenkin Hospital, Osaka, Japan

Y. Inui
Hyogo Prefectural Nishinomiya Hospital, Nishinomiya, Japan

H. Fukui
Yao Municipal Hospital, Osaka, Japan

T. Hijioka
National Hospital Organization Osaka Minami Medical Center, Kawachinagano, Japan

K. Katayama
Osaka Medical Center for Cancer and Cardiovascular Diseases, Osaka, Japan

S. Tamura
Minoh City Hospital, Minoh, Japan

H. Yoshihara
Osaka Rousai Hospital, Sakai, Japan

A. Inoue
Osaka General Medical Center, Osaka, Japan

Y. Imai
Ikeda Municipal Hospital, Ikeda, Japan

E. Hayashi
Kinki Central Hospital of Mutual Aid Association of Public School Teachers, Itami, Japan

M. Kato
National Hospital Organization Minami Wakayama Medical Center, Tanabe, Japan

decreases ($p < 0.001$); no patient without a p-EVR in the previous treatment attained an SVR with re-treatment (0/16). All patients with <5 $\log_{10}$ IU/ml of HCV RNA at the start of re-treatment attained an SVR (6/6), while only 33% (15/45) of those patients with ≥5 $\log_{10}$ IU/ml of HCV RNA attained an SVR ($p < 0.01$). Among the patients with relapse in the previous treatment, those who attained an SVR on re-treatment required a longer duration of re-treatment than the duration of the previous treatment (re-treatment, 63.8 ± 13.0 weeks vs. previous treatment, 53.9 ± 13.5 weeks, $p = 0.01$).

Conclusions Re-treatment of genotype 1 patients should be limited to patients with a p-EVR in the previous treatment and a low HCV RNA level at the start of re-treatment. In re-treatment with Peg-IFN plus ribavirin, longer treatment duration can contribute to increasing the anti-viral effect.

Keywords Chronic hepatitis C · Pegylated interferon and ribavirin combination therapy · Re-treatment

Introduction

Pegylated interferon (Peg-IFN) plus ribavirin combination therapy can improve anti-viral efficacy and is currently recommended as first-line therapy for chronic hepatitis C. However, hepatitis C virus (HCV) still persists in approximately half of the genotype 1 patients treated with Peg-IFN plus ribavirin [1–4], and the number of patients who fail to achieve a sustained virologic response (SVR) consequently increases over time.

Recently, the addition of a protease inhibitor to Peg-IFN plus ribavirin combination therapy has been reported to improve the anti-viral effect, but this triple therapy increases side effects, especially severe anemia [5–7]. In Japan, HCV carriers are 10–20 years older than those in the United States and European countries, and patients who are ineligible for triple therapy exist in large numbers due to their potential tendency of having anemia. On the other hand, re-treatment with Peg-IFN plus ribavirin is a possible choice, until triple therapy becomes commercially available, for patients who have failed to show an SVR to previous anti-viral therapy, and for patients who are ineligible for triple therapy. As for re-treatment with Peg-IFN plus ribavirin, there have been only a few studies of patients who failed to show an SVR to previous Peg-IFN plus ribavirin [8–11]. Although re-treatment with Peg-IFN plus ribavirin for patients who failed to respond to previous Peg-IFN plus ribavirin is not recommended in the practice guidelines of the American Association for the Study of the Liver (AASLD) [1], there are some patients who respond to re-treatment. However, it remains obscure in which patients eradication of HCV can be successfully attained by re-treatment with Peg-IFN plus ribavirin.

In the present study, we tried to determine which patients could benefit from re-treatment and to identify the factors associated with an SVR in re-treatment.

Patients and methods

Patients

The present study was a retrospective, multicenter trial conducted by Osaka University Hospital and other institutions participating in the Osaka Liver Forum. This study was conducted with 74 chronic hepatitis C patients (genotype 1, $n = 56$, genotype 2, $n = 18$) who had previously completed Peg-IFN α-2b plus ribavirin combination therapy but had failed to attain an SVR. Patients were excluded from this study if they had decompensated cirrhosis or other forms of liver disease (alcoholic liver disease, autoimmune hepatitis), or coinfection with hepatitis B or anti-human immunodeficiency virus. This study was conducted according to the ethical guidelines of the Declaration of Helsinki amended in 2008, and informed consent was obtained from each patient.

Treatment

For the previous treatment, Peg-IFN α-2b (Pegintron; Schering-Plough, Kenilworth, NJ, USA) plus ribavirin (Rebetol; Schering-Plough) was started between December 2004 and January 2008. For re-treatment with Peg-IFN plus ribavirin, Peg-IFN α-2a (Pegasys; Roche, Basel, Switzerland) plus ribavirin (Copegus; Roche) or Peg-IFN α-2b plus ribavirin was started between February 2006 and January 2009. In principle, as a starting dose, Peg-IFN was given once weekly at a dose of 180 μg of Peg-IFN α-2a and 1.5 μg/kg of Peg-IFN α-2b, and ribavirin was given at a total dose of 600–1000 mg/day based on body weight (for genotype 1, body weight <60 kg, 600 mg; 60–80 kg, 800 mg; >80 kg, 1000 mg; for genotype 2, body weight <60 kg, 600 mg; >60 kg, 800 mg), according to a standard treatment protocol for Japanese patients.

Dose reduction and discontinuance

Dose modification followed, as a rule, the manufacturer's drug information on the intensity of the hematologic adverse effects. The Peg-IFN α-2a and α-2b doses were reduced to 50% of the assigned dose when the neutrophil count fell below 750/mm^3 or the platelet (Plt) count fell below 8×10^4/mm^3, and the agent was discontinued when the neutrophil count fell below 500/mm^3 or the Plt count fell below 5×10^4/mm^3. Ribavirin was also reduced from 1000 to 600, 800 to 600, or 600 to 400 mg when the

hemoglobin (Hb) was below 10 g/dl, and was discontinued when the Hb was below 8.5 g/dl. Both Peg-IFN and ribavirin had to be discontinued if there was a need to discontinue one of the drugs. No iron supplement or hematopoietic growth factors, such as epoietin alpha or granulocyte–macrophage colony stimulating factor (G-CSF), were administered.

Virologic assessment and definition of virologic response

The serum HCV RNA level was quantified using the COBAS AMPLICOR HCV MONITOR test, version 2.0 (detection range 6–5000 KIU/ml; Roche Diagnostics, Branchburg, NJ, USA) and qualitatively analyzed using the COBAS AMPLICOR HCV test, version 2.0 (lower limit of detection 50 IU/ml). A rapid virologic response (RVR) was defined as undetectable serum HCV RNA level at week 4, a partial early virologic response (p-EVR) was defined as more than a 2-log decrease in HCV RNA level at week 12 compared with the baseline, a complete EVR (c-EVR) was defined as undetectable serum HCV RNA at week 12, a late virologic response (LVR) was defined as detectable serum HCV RNA at week 12 and undetectable at week 24, and an SVR was defined as undetectable serum HCV RNA at 24 weeks after the end of the treatment. Relapse was defined as undetectable serum HCV RNA at the end of the treatment but a detectable amount after the end of the treatment. For both the previous treatment and this re-treatment, patients without a p-EVR or without clearance of HCV RNA at week 24 were considered to be showing non-response (NR) and had to stop treatment. A patient who attained HCV RNA negativity during the re-treatment continued to be treated for 48 or 72 weeks according to response-guided therapy and the decision of the investigator at the participating clinical center.

Statistical analysis

Baseline data of the patients are expressed as mean ± SD or median values. In order to analyze the differences between baseline data or the factors associated with SVR, univariate analysis using the Mann–Whitney *U*-test or the χ^2 test was performed. A two-tailed p value of <0.05 was considered significant. The analysis was conducted with SPSS version 15.0J (SPSS, Chicago, IL, USA).

Results

The baseline characteristics of the patients are summarized in Table 1. Of the 56 genotype 1 patients, 32 were relapsers and 24 showed NR to previous treatment. Among the relapsers, 15 had shown a c-EVR (58%, 15/26) and 29 a p-EVR (100%, 29/29) in the previous treatment. Of the 18 genotype 2 patients, 17 were relapsers and one had shown NR to the previous treatment. Among the relapsers, 5 had shown an RVR (42%, 5/12) in the previous treatment. In the previous treatment, all patients had received Peg-IFN α-2b plus RBV combination therapy. There were no significant differences among the baseline characteristics between the previous treatment and the re-treatment in

Table 1 Baseline characteristics of patients and treatment factors in previous treatment and re-treatment

	Genotype 1						Genotype 2	
	All patients		Previous treatment relapsers		Previous treatment non-responders		All patients	
Number of patients	56		32		24		18	
Sex: male/female	32/24		19/13		13/11		11/7	
	Previous treatment	Re-treatment	Previous treatment	Re-treatment	Previous treatment	Re-treatment	Previous treatment	Re-treatment
Age (years)	57.6 ± 9.2	59.5 ± 9.4	57.8 ± 9.0	59.8 ± 9.4	57.3 ± 9.6	59.0 ± 9.5	57.4 ± 9.0	58.4 ± 1.7
White blood cells (/mm^3)	4909 ± 1404	4670 ± 1566	5117 ± 1276	4756 ± 979	4633 ± 1543	4545 ± 2178	5111 ± 1697	4412 ± 1744
Red blood cells (×10^4/mm^3)	435 ± 40	426 ± 52	444 ± 34	437 ± 36	4243 ± 46	412 ± 67	448 ± 36	447 ± 38
Hemoglobin (g/dl)	13.9 ± 1.2	13.5 ± 1.7	14.1 ± 1.1	13.8 ± 1.3	13.7 ± 1.3	13.1 ± 2.1	14.4 ± 1.2	14.2 ± 1.3
Platelets (×10^4/mm^3)	16.5 ± 6.1	17.5 ± 6.9	18.4 ± 6.6	19.1 ± 6.5	14.1 ± 4.4	15.2 ± 6.9	17.5 ± 6.3	16.2 ± 4.9
AST (IU/l)	58 ± 30	60 ± 45	55 ± 31	56 ± 44	61 ± 28	64 ± 47	52 ± 34	34 ± 13
ALT (IU/l)	74 ± 55	77 ± 74	73 ± 65	79 ± 80	74 ± 40	75 ± 66	65 ± 52	34 ± 18
Serum HCV RNA (KIU/ml)	1600	1100	1600	1100	1600	990	1300	690
Peg-IFN type: α2a/α2b	0/56	24/32	0/32	14/18	0/24	10/14	0/18	4/14

AST aspartate aminotransferase, *ALT* alanine aminotransferase, *HCV* hepatitis C virus, *Peg-IFN* pegylated interferon

Table 2 Factors associated with a sustained virologic response (SVR) in re-treatment with Peg-IFN plus ribavirin

Factor	SVR	Non-SVR	*p* value
Number of patients	23	33	
Age (years)	59.5 ± 7.6	59.5 ± 10.5	0.55
Sex: male/female	16/7	16/17	0.17
White blood cells (/mm^3)	4778 ± 1022	4589 ± 1884	0.29
Neutrophils (/mm^3)	2446 ± 849	2291 ± 1486	0.21
Hemoglobin (g/dl)	13.6 ± 1.3	13.4 ± 1.9	0.73
Platelets (×10^4/mm^3)	18.2 ± 6.3	16.9 ± 7.3	0.28
AST (IU/l)	52 ± 33	65 ± 52	0.46
ALT (IU/l)	75 ± 61	79 ± 82	0.72
Serum HCV RNA: <5log/5log≤	6/15	0/31	<0.01
Peg-IFN type: α2a/α2b	7/16	17/16	0.27
Peg-IFN dose (μg/kg/week)			
α2a	2.64 ± 0.61	2.73 ± 0.72	0.90
α2b	1.18 ± 0.43	1.19 ± 0.34	0.90
Ribavirin dose (mg/kg/day)	8.6 ± 2.9	9.4 ± 2.7	0.28
1st treatment virologic response			
p-EVR; +/−	22/0	14/16	<0.001
Relapse/NR	20/3	12/21	<0.001

p-EVR partial early virologic response, *NR* non-response

terms of peripheral blood cell counts, or the levels of aminotransaminases and serum HCV RNA at the start of treatment.

In genotype 1 patients, the HCV RNA negative rate on re-treatment was 54% (29/54) at week 12 and 71% (40/56) at week 24, and the SVR rate was 41% (23/56). The factors associated with SVR were assessed by univariate analysis for the following variables; age, gender, peripheral blood cell counts, aminotransferases, previous treatment response, serum HCV RNA level, the type of Peg-IFN in re-treatment, and drug adherence (Table 2). As a result, the factors of previous treatment response and serum HCV RNA level at the start of re-treatment were selected as being significant. In examining the efficacy of the re-treatment according to the previous treatment response, the relapsers in the previous treatment had a significantly higher HCV RNA negative rate at weeks 12 and 24 and a significantly higher SVR rate than those with NR in the previous treatment (Fig. 1a). Patients with a p-EVR in the previous treatment showed similar results, while no patient without p-EVR in the previous treatment attained an SVR on re-treatment (0/16) (Fig. 1b). Even among the patients without HCV RNA negativity in the previous treatment, if p-EVR had been attained in the previous treatment, 43% (3/7) of these patients attained an SVR on re-treatment. As for the serum HCV RNA level at the start of re-treatment, all patients with less than 5 $\log_{10}$ IU/ml of HCV RNA attained an SVR (6/6), and 33% (15/45) of those patients with more than 5 $\log_{10}$ IU/ml of HCV RNA attained an SVR ($p < 0.01$).

In examining the efficacy of re-treatment according to treatment duration, among the patients with c-EVR and without RVR on re-treatment, those who were re-treated for 72 weeks tended to attain higher SVR rates than those who were re-treated for 48 weeks (72 weeks, 75%, 9/12, vs. 48 weeks, 25%, 2/8, $p = 0.06$). On the other hand, 43% (3/7) of the patients with an LVR on re-treatment attained an SVR on re-treatment. Among the patients with relapse

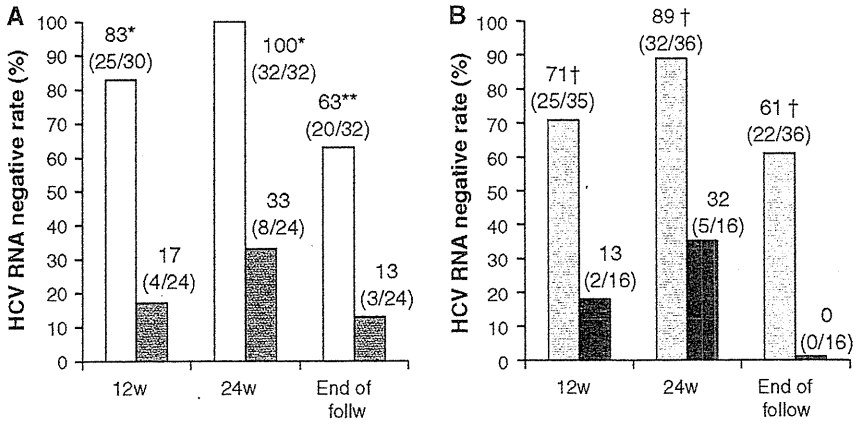

Fig. 1 Virologic response on re-treatment according to previous treatment response. **a** Hepatitis C virus (HCV) RNA negative rate on re-treatment according to relapse or non-response in previous treatment. **b** HCV RNA negative rate on re-treatment according to partial early virologic response (p-EVR) or non-p-EVR in previous treatment. *White bars* patients with relapse in previous treatment. *Dark gray bars* patients with non-response in previous treatment. *Light gray bars* patients with p-EVR in previous treatment. *Black bars* patients with non-p-EVR in previous treatment. *$p < 0.0001$; **$p < 0.01$; compared to non-response. †$p < 0.001$; compared to patients without p-EVR

in the previous treatment, those who attained an SVR on re-treatment required a longer duration of re-treatment than the duration of the previous treatment (re-treatment, 63.8 ± 13.0 weeks vs. previous treatment, 53.9 ± 13.5 weeks, $p = 0.01$), while those without an SVR on re-treatment could be treated for almost the same period as that in the previous treatment (re-treatment, 58.8 ± 12.8 weeks vs. previous treatment, 54.2 ± 11.3 weeks, $p = 0.38$).

Comparison of the timing to the first undetectable HCV RNA level in the previous treatment and re-treatment could be carried out in 50 patients; most patients attained HCV RNA negativity on re-treatment earlier or with the same timing as in the previous treatment, and only one patient showed a later timing for re-treatment. The SVR rate on re-treatment was low, at 13% (3/24) among the patients with detectable HCV RNA at week 24 in the previous treatment. Among the 10 patients with HCV RNA negativity on re-treatment with the same timing as that in the previous treatment, an SVR was attained only by the patients who were re-treated for 72 weeks. Among the 23 patients with earlier HCV RNA negativity on re-treatment, an SVR of 61% was attained (14/23). The patients with an RVR on re-treatment attained a high SVR rate (88%, 7/8) regardless of the virologic response in the previous treatment (Fig. 2).

In genotype 2 patients, the HCV RNA negative rate on re-treatment was 56% (10/18) at week 4, 83% (15/18) at week 12, and 89% (16/18) at week 24, and the SVR rate was 56% (10/18). The two patients without a c-EVR in the previous treatment did not attain an SVR on re-treatment. Among the patients with an RVR on re-treatment, the SVR rates were 60% (3/5) in those with 24-week treatment and 100% (5/5) in those with 48-week treatment.

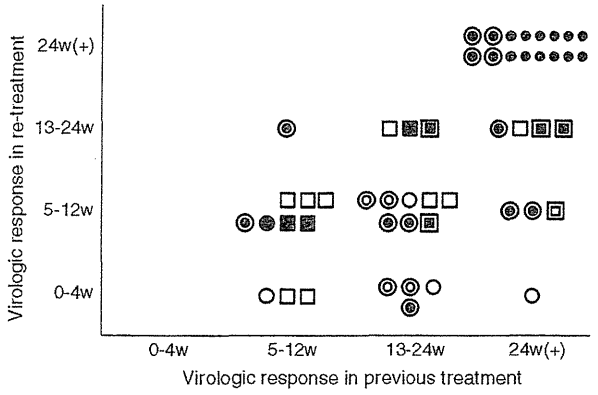

Fig. 2 Virologic response on re-treatment according to the timing of HCV RNA negativity in previous treatment and re-treatment. *Open double circles/open circles* sustained virologic response (SVR) with 48 weeks of re-treatment (*open double circles*, pegylated interferon [Peg-IFN] α-2a plus ribavirin; *open circles* Peg-IFN α-2b plus ribavirin). *Open double squares/open squares*, SVR with 72 weeks of re-treatment (*open double squares* Peg-IFN α-2a plus ribavirin; *open squares*, Peg-IFN α-2b plus ribavirin). *Closed double circles/closed circles*, non-SVR with 48 weeks of re-treatment or non-response (NR) with 24 weeks of re-treatment (*closed double circles*, Peg-IFN α-2a plus ribavirin; *closed circles* Peg-IFN α-2b plus ribavirin). *Closed double squares/closed squares*, non-SVR with 72 weeks of re-treatment (*closed double squares* Peg-IFN α-2a plus ribavirin; *closed squares*, Peg-IFN α-2b plus ribavirin)

Discussion

In the present study of the re-treatment of chronic hepatitis C patients who failed to show an SVR to Peg-IFN plus ribavirin therapy, the patients with relapse in the previous treatment showed a significant response on re-treatment compared with those with NR. This result showed similar findings to the evaluation of peg intron in control of hepatitis C chirrosis (EPIC) study of relapse and NR [10]. In addition, in the present study, p-EVR in the previous treatment was a good indicator of negative prediction for SVR on re-treatment; no patient without p-EVR in the previous treatment attained SVR on re-treatment; that is, the negative predictive value for SVR on re-treatment was 100%. Recently, genetic polymorphism near the IL28B gene has been reported to be associated with the anti-viral effect of Peg-IFN plus ribavirin combination therapy [12–15]. Among Japanese genotype 1 patients, it has been reported that those with the major single-nucleotide polymorphism (SNP) allele of IL28B (rs8099917) show an SVR rate of 39%, while those with the minor allele show an SVR rate of only 11%. Hence, in re-treatment for patients who failed to show a SVR to Peg-IFN plus ribavirin therapy, pretreatment prediction should be done by taking IL28B SNPs and the previous treatment response into account. Patients with the minor SNP allele of IL28B s who did not attain a p-EVR in the previous treatment should wait until new drugs become commercially available.

The next question is how the patients should be re-treated in order to attain an SVR on re-treatment. In the present study, the patients with a low serum HCV RNA level (less than 5 $\log_{10}$ IU/ml) at the start of re-treatment showed a significant rate of cure on re-treatment, and this is almost the same result as that previously reported [9, 10]. In the present study, one patient with NR in the previous treatment started re-treatment with HCV RNA of 52 KIU/ml and attained an RVR and SVR. HCV RNA levels declined on re-treatment among 61% (34/56) of the patients compared to the start of the previous treatment, and it is important not to miss the timing of when the HCV RNA level is low.

With respect to treatment duration among patients with HCV RNA negativity during re-treatment, 72 weeks of treatment tended to increase the SVR rate compared to

48 weeks of treatment (72 weeks, 68%, 15/22, vs. 48 weeks, 44%, 7/16, $p = 0.13$). This result was almost the same as that of the re-treatment of patients with chronic hepatitis C who do not respond to peginterferon-alpha 2b. A randomized trial (REPEAT) study [9]. Furthermore, in the present study, among the patients with relapse in the previous treatment, those who attained an SVR on re-treatment required a longer re-treatment duration than the duration of the previous treatment. In fact, the longer treatment brought about an SVR in some patients whose timing of HCV RNA negativity on re-treatment was the same as that in the previous treatment, as shown in Fig. 2. Thus, especially to be noted is that the relapsers in the previous treatment should be re-treated for a longer period than that of the previous treatment.

It has been reported that splenectomy and partial splenic embolization (PSE) are considered to make it possible for patients with cirrhosis and thrombocytopenia to initiate and continue anti-viral therapy safely, by increasing the platelet counts [16–19]. If poor adherence and inappropriate duration have contributed to a poor response in previous treatment due to thrombocytopenia, there is a possibility that increasing the platelet counts by splenectomy or PSE contributes to improving the tolerability of and adherence to re-treatment, and to increasing the SVR rate in re-treatment. In the present study, one patient with cirrhosis and thrombocytopenia who showed NR in the previous treatment owing to poor adherence to the Peg-IFN α-2b (0.78 μg/kg) regimen underwent splenectomy before re-treatment. As a result, the patient could continue with a sufficient dose of Peg-IFN (1.53 μg/kg) in the re-treatment and attained HCV negativity at re-treatment week 24 and an SVR by extended treatment. Further study is needed on the issue of the effect of splenectomy or PSE in re-treatment on the efficacy of re-treatment with Peg-IFN plus ribavirin therapy.

In the present study, the SVR rate was relatively high (56%) in patients with genotype 2. The patients who could not attain SVR on re-treatment (2 patients) had not attained a c-EVR in the previous treatment. And, among the patients with an RVR on re-treatment, all patients treated for 48 weeks attained an SVR (5 patients), while 40% (2/5) of patients treated for 24 weeks could not attain an SVR. Thus, in patients with genotype 2, as well as in those with genotype 1, the previous treatment response and response-guided therapy can be useful in decisions on the indication for re-treatment or the treatment duration on re-treatment. However, in this study, detailed analysis was not possible because of the small number of genotype 2 patients. Further investigation is needed to clarify this.

The limitation of the present study was that two types of Peg-IFN were used. As for the type of Peg-IFN, some reports have suggested that Peg-IFN α-2a has a stronger anti-viral effect than Peg-IFN α-2b [20, 21], and others have suggested that the two types of Peg-IFN have an almost equal anti-viral effect [22]. In this study, the HCV RNA negative rate at re-treatment week 12 was similar (α-2a, 59%, 13/22, vs. α-2b, 50%, 16/32, $p = 0.51$) between the patients with Peg-IFN α-2a and those with Peg-IFN α-2b. Furthermore, among 24 patients treated with Peg-IFN α-2a on re-treatment, an SVR rate of 38% was attained with 48-week treatment and an SVR rate of 60% was attained with 72-week treatment among patients with a p-EVR in the previous treatment, but no patient without a p-EVR in the previous treatment attained an SVR on re-treatment. Similarly, among 32 patients treated with Peg-IFN α-2b in re-treatment, an SVR rate of 56% was attained with 48-week treatment and an SVR rate of 79% was attained with 72-week treatment among patients with a p-EVR in the previous treatment, but no patient without a p-EVR in the previous treatment attained an SVR on re-treatment. As noted above, since the virologic responses to both Peg-IFNs among re-treated patients were similar, in this study we analyzed the effect of re-treatment without distinction of the type of Peg-IFN.

In conclusion, our results have demonstrated that the efficacy of re-treatment for genotype 1 patients who failed to show an SVR to previous treatment with Peg-IFN plus ribavirin could be predicted by the previous treatment response, especially in terms of p-EVR and a low HCV RNA level at the start of re-treatment. Re-treatment for 72 weeks led to clinical improvement for genotype 1 patients who attained HCV RNA negativity on re-treatment.

Acknowledgments Other institutions and participants in the Osaka Liver Forum are: Higashiosaka City Central Hospital, S Iio; Itami City Hospital, Y Saji; Toyonaka Municipal Hospital, M Inada; Otemae Hospital, Y Doi; Suita Municipal Hospital, T Nagase; NTT West Osaka Hospital, A Kaneko; Ashiya Municipal Hospital, T Kitada; Nishinomiya Municipal Central Hospital, H Ogawa; Saiseikai Senri Hospital, K Suzuki; Izumiotsu Municipal Hospital, S Yamagata; Osaka Kaisei Hospital, N Imaizumi; Kano General Hospital, S Kubota; Saso Hospital, M Nishiuchi; and Meiwa Hospital, Y Hayakawa. This work was supported by a Grant-in-Aid for Research on Hepatitis and BSE from the Ministry of Health, Labour and Welfare of Japan, and Scientific Research from the Ministry of Education, Science, and Culture of Japan. All authors have no financial relationships relevant to this study.

References

1. Ghany MG, Strader DB, Thomas DL, Seeff LB. Diagnosis, management, and treatment of hepatitis C: an update. Hepatology. 2009;49:1335–74.
2. Hayashi N, Takehara T. Antiviral therapy for chronic hepatitis C: past, present, and future. J Gastroenterol. 2006;41:17–27.
3. Manns MP, McHutchison JG, Gordon SC, Rustgi VK, Shiffman M, Reindollar R, et al. Peginterferon alfa-2b plus ribavirin

compared with interferon alfa-2b plus ribavirin for initial treatment of chronic hepatitis C: a randomised trial. Lancet. 2001;358:958–65.
4. Fried MW, Shiffman ML, Reddy KR, Smith C, Marinos G, Goncales FL Jr, et al. Peginterferon alfa-2a plus ribavirin for chronic hepatitis C virus infection. N Engl J Med. 2002;347:975–82.
5. McHutchison JG, Everson GT, Gordon SC, Jacobson IM, Sulkowski M, Kauffman R, et al. Telaprevir with peginterferon and ribavirin for chronic HCV genotype 1 infection. N Engl J Med. 2009;360:1827–38.
6. Hezode C, Forestier N, Dusheiko G, Ferenci P, Pol S, Goeser T, et al. Telaprevir and peginterferon with or without ribavirin for chronic HCV infection. N Engl J Med. 2009;360:1839–50.
7. McHutchison JG, Manns MP, Muir AJ, Terrault NA, Jacobson IM, Afdhal NH, et al. Telaprevir for previously treated chronic HCV infection. N Engl J Med. 2010;362:1292–303.
8. Bacon BR, Shiffman ML, Mendes F, Ghalib R, Hassanein T, Morelli G, et al. Retreating chronic hepatitis C with daily interferon alfacon-1/ribavirin after nonresponse to pegylated interferon/ribavirin: DIRECT results. Hepatology. 2009;49:1838–46.
9. Jensen DM, Marcellin P, Freilich B, Andreone P, Di Bisceglie A, Brandao-Mello CE, et al. Re-treatment of patients with chronic hepatitis C who do not respond to peginterferon-alpha2b: a randomized trial. Ann Intern Med. 2009;150:528–40.
10. Poynard T, Colombo M, Bruix J, Schiff E, Terg R, Flamm S, et al. Peginterferon alfa-2b and ribavirin: effective in patients with hepatitis C who failed interferon alfa/ribavirin therapy. Gastroenterology. 2009;136:1618–28.
11. Berg C, Goncales FL Jr, Bernstein DE, Sette H Jr, Rasenack J, Diago M, et al. Re-treatment of chronic hepatitis C patients after relapse: efficacy of peginterferon-alpha-2a (40 kDa) and ribavirin. J Viral Hepat. 2006;13:435–40.
12. Thomas DL, Thio CL, Martin MP, Qi Y, Ge D, O'Huigin C, et al. Genetic variation in IL28B and spontaneous clearance of hepatitis C virus. Nature. 2009;461:798–801.
13. Suppiah V, Moldovan M, Ahlenstiel G, Berg T, Weltman M, Abate ML, et al. IL28B is associated with response to chronic hepatitis C interferon-alpha and ribavirin therapy. Nat Genet. 2009;41:1100–4.
14. Tanaka Y, Nishida N, Sugiyama M, Kurosaki M, Matsuura K, Sakamoto N, et al. Genome-wide association of IL28B with response to pegylated interferon-alpha and ribavirin therapy for chronic hepatitis C. Nat Genet. 2009;41:1105–9.
15. Thompson AJ, Muir AJ, Sulkowski MS, Ge D, Fellay J, Shianna KV, et al. Interleukin-28B polymorphism improves viral kinetics and is the strongest pretreatment predictor of sustained virologic response in hepatitis C virus-1 patients. Gastroenterology. 2010;139:120–9.
16. Hayashi PH, Mehia C, Joachim Reimers H, Solomon HS, Bacon BR. Splenectomy for thrombocytopenia in patients with hepatitis C cirrhosis. J Clin Gastroenterol. 2006;40:740–4.
17. Miyake Y, Ando M, Kaji E, Toyokawa T, Nakatsu M, Horihata M. Partial splenic embolization prior to combination therapy of interferon and ribavirin in chronic hepatitis C patients with thrombocytopenia. Hepatol Res. 2008;38:980–6.
18. Morihara D, Kobayashi M, Ikeda K, Kawamura Y, Saneto H, Yatsuji H, et al. Effectiveness of combination therapy of splenectomy and long-term interferon in patients with hepatitis C virus-related cirrhosis and thrombocytopenia. Hepatol Res. 2009;39:439–47.
19. Ikezawa K, Naito M, Yumiba T, Iwahashi K, Onishi Y, Kita H, et al. Splenectomy and antiviral treatment for thrombocytopenic patients with chronic hepatitis C virus infection. J Viral Hepat. 2010;17:488–92.
20. Ascione A, De Luca M, Tartaglione MT, Lampasi F, Di Costanzo GG, Lanza AG, et al. Peginterferon alfa-2a plus ribavirin is more effective than peginterferon alfa-2b plus ribavirin for treating chronic hepatitis C virus infection. Gastroenterology. 2010;138:116–22.
21. Awad T, Thorlund K, Hauser G, Stimac D, Mabrouk M, Gluud C. Peginterferon alpha-2a is associated with higher sustained virological response than peginterferon alfa-2b in chronic hepatitis C: systematic review of randomized trials. Hepatology. 2010;51:1176–84.
22. McHutchison JG, Lawitz EJ, Shiffman ML, Muir AJ, Galler GW, McCone J, et al. Peginterferon alfa-2b or alfa-2a with ribavirin for treatment of hepatitis C infection. N Engl J Med. 2009;361:580–93.

Increases in p53 expression induce CTGF synthesis by mouse and human hepatocytes and result in liver fibrosis in mice

Takahiro Kodama,[1] Tetsuo Takehara,[1] Hayato Hikita,[1] Satoshi Shimizu,[1] Minoru Shigekawa,[1] Hinako Tsunematsu,[1] Wei Li,[1] Takuya Miyagi,[1] Atsushi Hosui,[1] Tomohide Tatsumi,[1] Hisashi Ishida,[1] Tatsuya Kanto,[1] Naoki Hiramatsu,[1] Satoshi Kubota,[2] Masaharu Takigawa,[2] Yoshito Tomimaru,[3] Akira Tomokuni,[3] Hiroaki Nagano,[3] Yuichiro Doki,[3] Masaki Mori,[3] and Norio Hayashi[4]

[1]Department of Gastroenterology and Hepatology, Osaka University Graduate School of Medicine, Suita, Osaka, Japan. [2]Department of Biochemistry and Molecular Dentistry, Okayama University Graduate School of Medicine, Dentistry and Pharmaceutical Sciences, Okayama, Japan. [3]Department of Surgery, Osaka University Graduate School of Medicine, Suita, Osaka, Japan. [4]Kansai-Rosai Hospital, Amagasaki, Hyogo, Japan.

The tumor suppressor p53 has been implicated in the pathogenesis of non-cancer-related conditions such as insulin resistance, cardiac failure, and early aging. In addition, accumulation of p53 has been observed in the hepatocytes of individuals with fibrotic liver diseases, but the significance of this is not known. Herein, we have mechanistically linked p53 activation in hepatocytes to liver fibrosis. Hepatocyte-specific deletion in mice of the gene encoding Mdm2, a protein that promotes p53 degradation, led to hepatocyte synthesis of connective tissue growth factor (CTGF; the hepatic fibrogenic master switch), increased hepatocyte apoptosis, and spontaneous liver fibrosis; concurrent removal of *p53* completely abolished this phenotype. Compared with wild-type controls, mice with hepatocyte-specific *p53* deletion exhibited similar levels of hepatocyte apoptosis but decreased liver fibrosis and hepatic CTGF expression in two models of liver fibrosis. The clinical significance of these data was highlighted by two observations. First, p53 upregulated CTGF in a human hepatocellular carcinoma cell line by repressing miR-17-92. Second, human liver samples showed a correlation between CTGF and p53-regulated gene expression, which were both increased in fibrotic livers. This study reveals that p53 induces CTGF expression and promotes liver fibrosis, suggesting that the p53/CTGF pathway may be a therapeutic target in the treatment of liver fibrosis.

Introduction

The tumor suppressor p53 primarily functions as a guardian of the genome, suppressing tumor development in various organs. In response to genotoxic stresses induced by DNA damage, reactive oxygen species, oncogene activation, and hypoxia, the p53 protein is stabilized and becomes transcriptionally active, leading to cell cycle arrest, DNA repair, and apoptosis predominantly through expression of p53-regulated genes such as *p21*, *PUMA*, *NOXA*, and *BAX* (1). Aside from these well-established roles, recent reports have revealed new aspects of p53, e.g., regulation of multiple biological functions such as glycolysis (2), anti-oxidation (3), autophagy (4), and senescence (5). It has also been demonstrated that p53 activation causes insulin resistance (6), cardiac failure (7), and early aging (5), indicating that p53 is involved even in the pathophysiology of various non-tumorous conditions via its numerous functions.

Organ fibrosis is considered to be a major medical issue, as various organs are involved, such as the liver, lung, heart, kidney, and skin, and its progression leads to organ failure and, especially in the liver, tumor development. The molecular mechanism of organ fibrosis has not yet been comprehensively clarified due to its complexity, and thus far, whether p53 is directly involved in its pathophysiology has not been addressed. Recently, p53 has been shown to accumulate in hepatocytes of several fibrotic liver diseases, such as non-alcoholic steatohepatitis (NASH) (8, 9), viral hepatitis (10, 11), and primary biliary cirrhosis (PBC) (12). However, the precise role of p53 in liver fibrosis is unclear. To this end, in the present study, we generated mice with hepatocyte-specific deletion of *Mdm2*, a critical p53 inhibitor, which strictly maintains p53 at a low level by promoting p53 degradation via the ubiquitin/proteasome pathway (13). Studies in these mice revealed that hepatocyte p53 activation caused spontaneous liver fibrosis. In addition to increased hepatocyte apoptosis, these mice showed hepatocyte upregulation of connective tissue growth factor (CTGF), known to be the fibrogenic master switch in fibrotic liver diseases (14). In vitro study revealed that p53 induced CTGF synthesis in hepatocytes via microRNA (miRNA) regulation. Hepatocyte-specific knockdown of *p53* attenuated CTGF expression and liver fibrosis induced by an atherogenic (ATH) diet or TAA injection. In human liver samples, p53-regulated gene expression increased in the fibrotic liver in correlation with an increase in *CTGF* gene expression. These findings demonstrated for the first time to our knowledge that p53 is directly involved in fibrogenesis in association with the induction of profibrogenic gene expression, suggesting that hepatocyte p53 activation and subsequent CTGF upregulation could be therapeutic targets in fibrotic liver disease.

Results

Hepatocyte-specific Mdm2 deficiency causes endogenous p53 accumulation, leading to transactivation of p53-regulated genes. To investigate the role of p53 in liver fibrosis, we first generated hepatocyte-specific Mdm2-knockout mice by crossing *Mdm2* floxed mice (*Mdm2*$^{fl/fl}$)

Authorship note: Takahiro Kodama and Tetsuo Takehara contributed equally to this work and share first authorship.

Conflict of interest: The authors have declared that no conflict of interest exists.

Citation for this article: *J Clin Invest.* 2011;121(8):3343–3356. doi:10.1172/JCI44957.

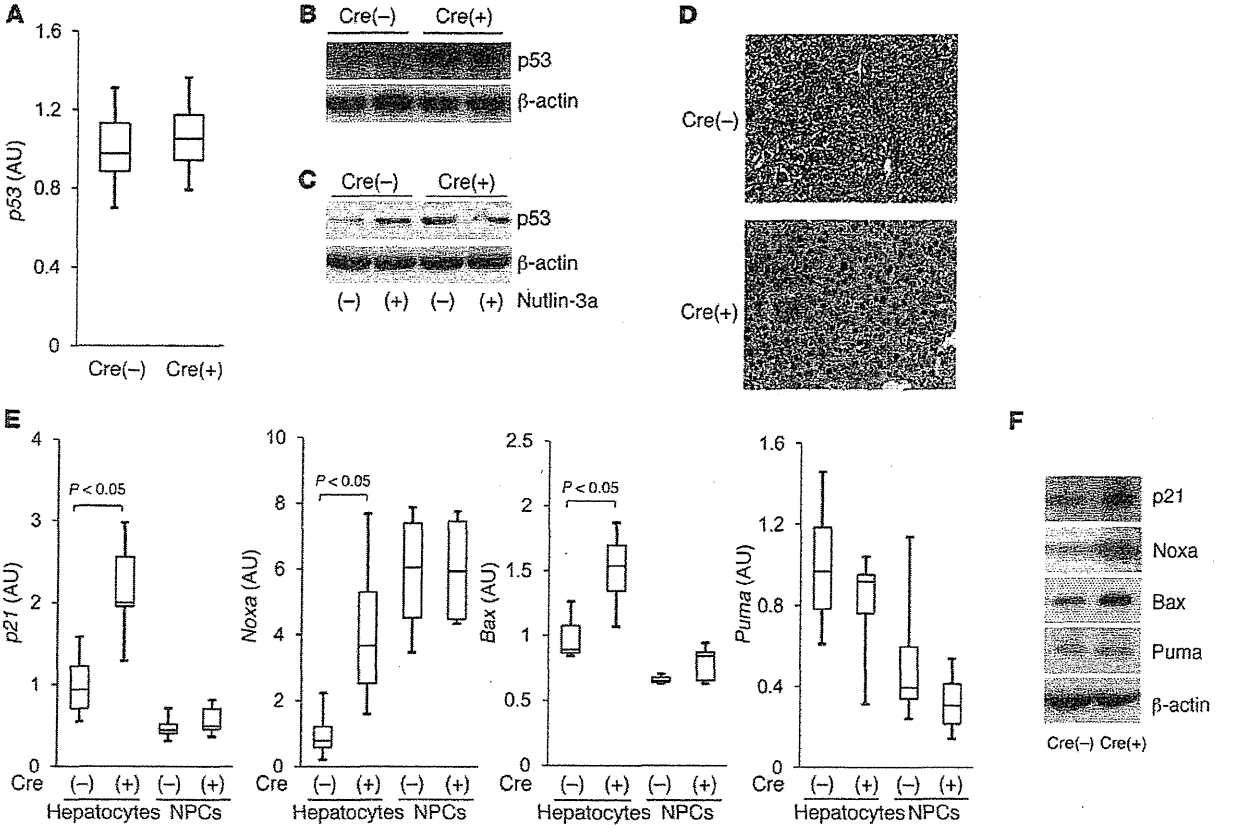

Figure 1

Hepatocyte-specific Mdm2-knockout mice show endogenous p53 accumulation, leading to transactivation of p53-regulated genes. (**A–F**) *Mdm2*$^{fl/fl}$*alb-cre* [Cre(+)] mice and *Mdm2*$^{fl/fl}$ [Cre(–)] mice were analyzed at 6 weeks of age. (**A**) *p53* mRNA levels in the liver tissue were determined by real-time RT-PCR; 7 mice per group. (**B**) Expression of p53 protein in liver tissue was assessed by Western blot analysis. (**C**) Expression of p53 protein in isolated hepatocytes upon treatment with 20 μM nutlin-3a or vehicle was assessed by Western blot analysis. (**D**) Expression of p53 protein in the liver section was determined by immunohistochemical analysis. Original magnification, ×200. (**E**) *p21*, *Noxa*, *Bax*, and *Puma* mRNA levels in isolated hepatocytes and NPCs were determined by real-time RT-PCR; 4 mice per group. Expression of p21, Noxa, Bax, and Puma proteins in liver tissue was assessed by Western blot analysis (**F**).

(15) and Alb-Cre transgenic mice (*alb-cre*) (16). After mating of *Mdm2*$^{fl/+}$*alb-cre* mice with *Mdm2*$^{fl/+}$ mice, *Mdm2*$^{fl/fl}$*alb-cre* mice were born at the expected Mendelian frequency and grew normally (Supplemental Figure 1; supplemental material available online with this article; doi:10.1172/JCI44957DS1). Next, we bred the *Mdm2*$^{fl/fl}$*alb-cre* mice with the *Mdm2*$^{fl/fl}$ mice and used *Mdm2*$^{fl/fl}$*alb-cre* mice as the knockout mice and *Mdm2*$^{fl/fl}$ mice as control littermates in the subsequent experiments. We examined whether Mdm2 deficiency would cause p53 accumulation in the liver. Real-time RT-PCR study revealed that hepatic levels of *p53* mRNA were not significantly different in the knockout mice and the control littermates (Figure 1A). Western blot analysis showed that hepatic p53 protein increased in the knockout mice compared with control littermates (Figure 1B). To determine whether an increase in p53 occurs in hepatocytes, we isolated hepatocytes from the liver by the collagenase-pronase perfusion procedure (17) and then examined their expression of p53 protein. Western blot analysis showed that the levels of hepatocyte p53 protein were higher in the knockout mice than in the control littermates (Figure 1C). These findings indicated that hepatocyte-specific Mdm2-knockout mice exhibited accumulation of p53 protein in their hepatocytes independent of the transcriptional upregulation of the *p53* gene. In addition, p53 expression increased in hepatocytes isolated from the control littermates, but not from the knockout mice, upon treatment with nutlin-3a, a small molecule Mdm2 inhibitor that blocks p53-Mdm2 interaction (ref. 18 and Figure 1C). This result demonstrated that lack of the Mdm2 function in hepatocytes of the knockout mice led to accumulation of endogenous p53 protein. Immunohistochemical examination of the liver sections revealed that p53 protein had accumulated in hepatocytes of the knockout mice, with some nuclear localization (Figure 1D), suggesting that p53 may become functionally active in hepatocytes of the knockout mice. This led us to investigate whether the p53 accumulation would lead to transactivation of p53-regulated genes *p21*, *Noxa*, *Bax*, and *Puma*. Real-time RT-PCR study revealed that, among these genes, the expression levels of *p21*, *Noxa*, and *Bax* was significantly higher in hepatocytes of the knockout mice than the control littermates (Figure 1E). Western blot study demonstrated that protein levels of these p53-regulated genes increased in the knockout mice as well (Figure 1F). These results demonstrated that hepatocyte-specific *Mdm2* deletion led to p53 accumulation and caused functional activation of p53 in hepatocytes.

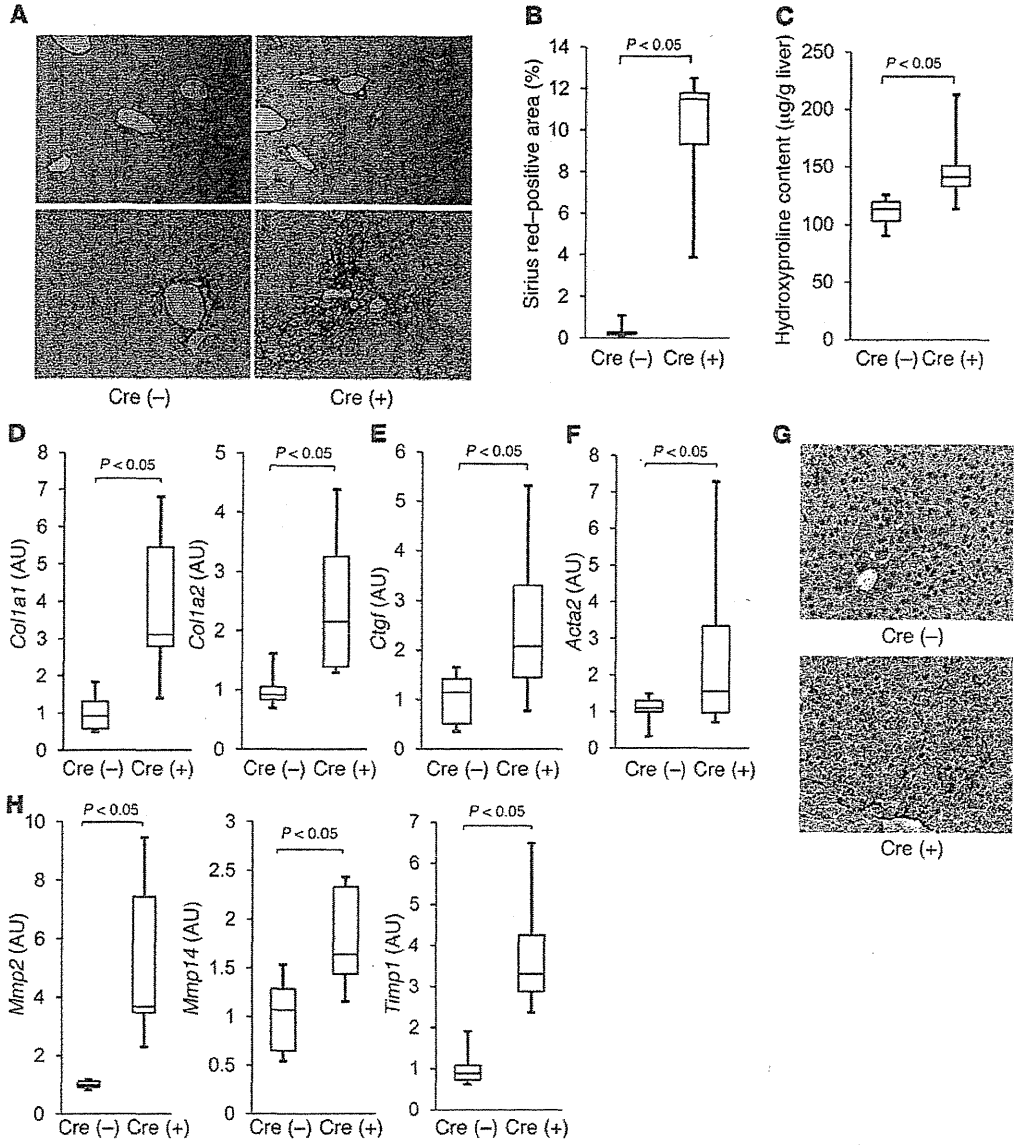

Figure 2

Hepatocyte-specific Mdm2-knockout mice develop spontaneous liver fibrosis with an increase in expression of the *Ctgf* gene. (**A–H**) *Mdm2*$^{fl/fl}$*alb-cre* [Cre(+)] mice and *Mdm2*$^{fl/fl}$ [Cre(–)] mice were analyzed at 6 weeks of age; 6 mice per group. (**A**) Liver fibrosis was evaluated by picrosirius red staining of liver sections (original magnification, upper panels, ×100; lower panels, ×200). (**B**) Sirius red–positive area of liver sections. (**C**) Hepatic hydroxyproline content. *Col1a1* and *Col1a2* (**D**), *Ctgf* (**E**), and *Acta2* (**F**) mRNA levels in the liver were determined by real time RT-PCR. (**G**) Expression of α-SMA in the liver sections was analyzed by immunohistochemistry. Original magnification, ×200. (**H**) *Mmp2*, *Mmp14*, and *Timp1* mRNA levels in the liver were determined by real time RT-PCR.

Hepatocyte-specific Mdm2-knockout mice develop spontaneous liver fibrosis with an increase in Ctgf gene expression. We next examined the consequences of hepatocyte p53 activation in the liver of Mdm2-knockout mice. To assess liver fibrosis, we evaluated hepatic collagen deposition by picrosirius red staining of liver tissues. At 6 weeks of age, pericellular and periportal bridging fibrosis was observed in liver of the knockout mice (Figure 2A), and it persisted even at a later time point (Supplemental Figure 2). Their collagen deposition significantly increased compared with that in the control littermates (Figure 2B). Hepatic hydroxyproline content, a biochemical marker of collagen accumulation (16), was also significantly higher in the knockout mice than in the wild-type mice (Figure 2C). We examined hepatic expression of the type I collagen genes *Col1a1* and *Col1a2* and found it to be significantly higher in the knockout mice than in the control littermates (Figure 2D). Among the major profibrogenic genes, real-time RT-PCR study revealed that hepatic expression of *Ctgf* was significantly higher in the knockout mice than in the control littermates (Figure 2E). Although *Tgfb1* and *Pdgfb* gene expression was slightly higher in the knockout mice than in the control litter-

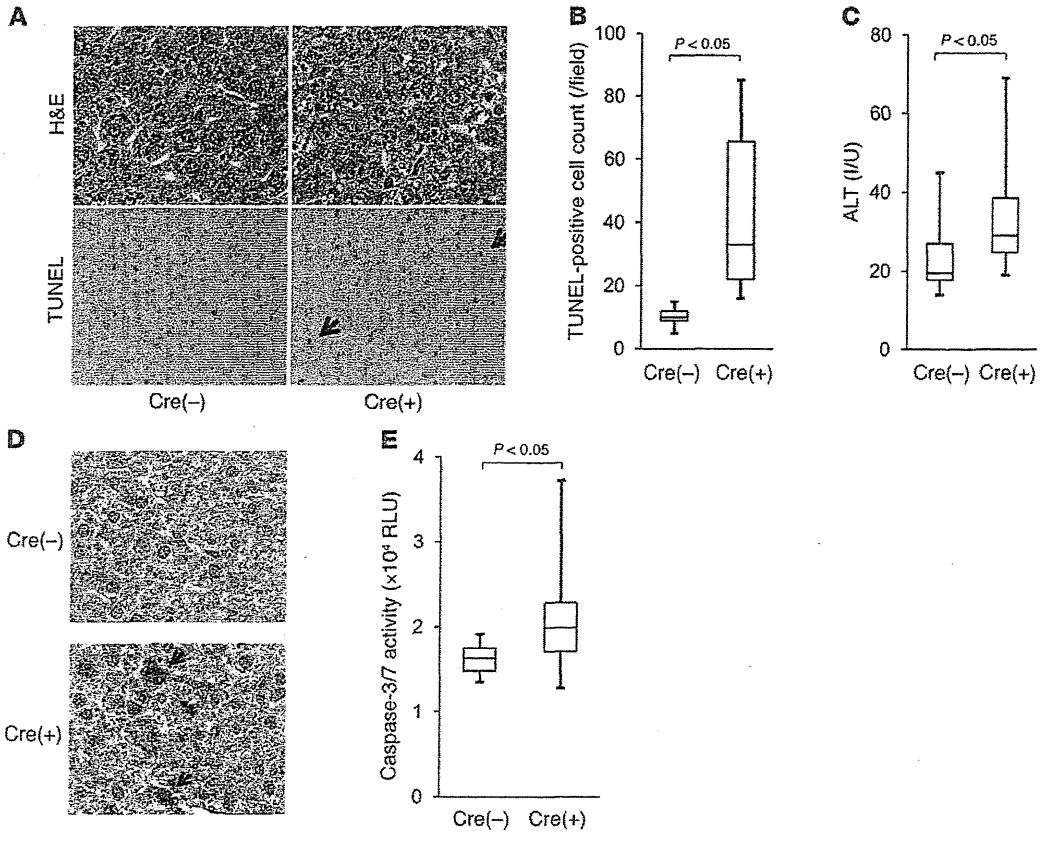

Figure 3

Hepatocyte-specific *Mdm2* deletion induces modest hepatocyte apoptosis. (**A–E**) *Mdm2*$^{fl/fl}$*alb-cre* [Cre(+)] mice and *Mdm2*$^{fl/fl}$ [Cre(–)] mice were examined at 6–8 weeks of age; more than 6 mice per group. (**A**) Hepatocyte apoptosis was evaluated by H&E staining and TUNEL staining of liver sections; black arrows indicate TUNEL-positive cells. Original magnification, upper panels, ×400; lower panels, ×200. (**B**) TUNEL-positive cell counts of liver sections. (**C**) Serum levels of ALT. (**D**) Expression of cleaved caspase-3 protein in the liver sections was assessed by immunohistochemistry; black arrows indicate cleaved caspase-3–positive cells. Original magnification, ×400. (**E**) Serum caspase-3/7 activity. RLU, relative light units.

mates, the difference was not significant (Supplemental Figure 3). These findings indicated that hepatocyte-specific *Mdm2* deletion led to spontaneous liver fibrosis with an increase in hepatic *Ctgf* gene expression. Activated hepatic stellate cells (HSCs), which express myogenic markers such as α-SMA, are major collagen-producing cells in the injured liver (19). We thus examined whether activated HSCs were involved in the spontaneous fibrosis of the knockout mice. Real time RT-PCR demonstrated that hepatic expression of the α-SMA gene *Acta2* was significantly higher in the knockout mice than in control littermates (Figure 2F), and immunohistochemical study revealed that α-SMA–positive cells increased in the liver of the knockout mice (Figure 2G), indicating that activated HSCs increased in the liver of the knockout mice. Liver fibrosis is known to be regulated by a fine balance between fibrogenesis and fibrinolysis, with activated HSCs playing a central role (19, 20). Real-time RT-PCR study showed that expression of fibrinolysis-related genes such as *Mmp2*, *Mmp14*, and *Timp1*, which are mainly produced from activated HSCs, also increased and was significantly higher in the knockout mice than in the control littermates (Figure 2H). These findings suggested the involvement of activated HSCs in regulation of the fibrosis phenotype in liver of the knockout mice.

Hepatocyte-specific Mdm2 deletion induces modest apoptosis, but regenerative capacity remains normal. p53 activation is known to induce apoptosis, cell-cycle arrest, and senescence in a variety of tissues (1). We examined apoptotic phenotypes in liver of the knockout mice. H&E staining of liver tissue revealed that a small number of hepatocytes with chromatin condensation and cytosolic shrinkage were scattered in the liver lobules of the knockout mice, with mild hepatic infiltration of inflammatory cells (Figure 3A). TUNEL staining of the liver tissue revealed an increase in TUNEL-positive cells in the knockout mice compared with the control littermates (Figure 3, A and B). Consistent with these histological observations, the levels of serum alanine aminotransferase (ALT), an indicator of liver injury, were slightly but significantly higher in the knockout mice than in the control littermates (Figure 3C). We also found that cleaved caspase-3, an active form of caspase-3, appeared in scattered hepatocytes of the knockout mice (Figure 3D), and that serum caspase-3/7 activity, which can be used as an indicator of hepatocyte apoptosis (21, 22), was significantly higher in the knockout mice than in the control littermates (Figure 3E). These findings indicated that hepatocyte-specific deletion of *Mdm2* led to a modest increase in spontaneous hepatocyte apoptosis. Next, we investigated the regenerative status of the liver upon 70% partial

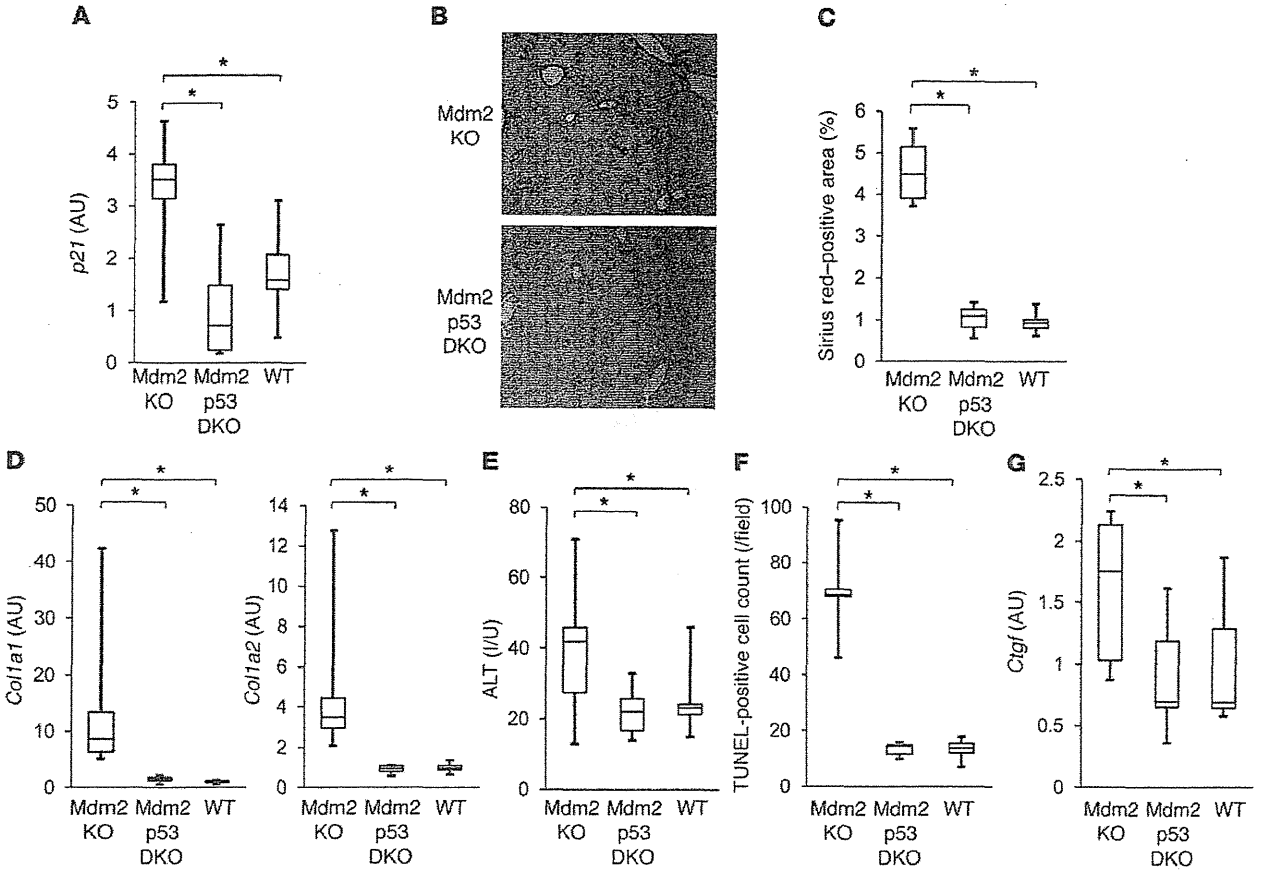

Figure 4

Spontaneous liver fibrosis in hepatocyte-specific Mdm2-knockout mice is completely abolished in a hepatocyte-specific p53-knockout background. (**A–G**) Offspring from mating of *Mdm2*$^{fl/fl}$*Trp53*$^{fl/+}$*alb-cre* mice and *Mdm2*$^{fl/fl}$*Trp53*$^{fl/+}$ mice were analyzed at 6 weeks of age; more than 5 mice per group. Mdm2 KO, *Mdm2*$^{fl/fl}$*Trp53*$^{+/+}$*alb-cre*; Mdm2 p53 DKO, *Mdm2*$^{fl/fl}$*trp53*$^{fl/fl}$*alb-cre*; WT, *Mdm2*$^{fl/fl}$*Trp53*$^{fl/fl}$ or *Mdm2*$^{fl/fl}$*Trp53*$^{+/+}$; *$P < 0.05$. (**A**) *p21* mRNA levels in the liver were determined by real-time RT-PCR. (**B**) Liver fibrosis was evaluated by picrosirius red staining of liver sections. Original magnification, ×100. (**C**) Sirius red–positive area of liver sections. (**D**) *Col1a1* and *Col1a2* mRNA levels in the liver were determined by real-time RT-PCR. (**E**) Serum levels of ALT. (**F**) Hepatocyte apoptosis was evaluated by TUNEL staining of liver sections. (**G**) *Ctgf* mRNA levels in the liver were determined by real-time RT-PCR. *$P < 0.05$.

hepatectomy, a well-established model of liver regeneration (23), by hepatic BrdU uptake and H&E staining of the liver tissue. Upon partial hepatectomy, compensatory liver regeneration occurred in both groups compared with the sham operation group, and the difference between them was not significant (Supplemental Figure 4, A and B). Even at a later time point, upon hepatectomy, liver volume steadily recovered in both groups and did not differ between them (Supplemental Figure 4C). These results indicated that hepatocyte-specific Mdm2 deficiency did not affect the regenerative capacity of the liver of the knockout mice. Senescence-associated β-galactosidase staining of the liver sections was also performed and showed that senescent hepatocytes were not obvious in both groups at 6 weeks of age (Supplemental Figure 5).

Spontaneous liver fibrosis in hepatocyte-specific Mdm2-knockout mice is abolished in a hepatocyte-specific p53-knockout background. To investigate whether p53 activation in hepatocytes is responsible for the phenotypes observed in the Mdm2-knockout mice, we generated hepatocyte-specific Mdm2- and p53-double-knockout mice by crossing hepatocyte-specific Mdm2-knockout mice (*Mdm2*$^{fl/fl}$*alb-cre*) and p53 floxed mice (*Trp53*$^{fl/fl}$). After mating of *Mdm2*$^{fl/fl}$*Trp53*$^{fl/+}$*alb-cre* mice with *Mdm2*$^{fl/fl}$*Trp53*$^{fl/+}$ mice, hepatocyte-specific Mdm2- and p53-double-knockout mice (*Mdm2*$^{fl/fl}$*Trp53*$^{fl/fl}$*alb-cre*) were born at the expected Mendelian frequency and grew normally (Supplemental Figure 6). Levels of the *p21* gene, as the p53-regulated gene, were significantly lower in the hepatocyte-specific Mdm2- and p53-double-knockout mice than in the hepatocyte-specific Mdm2-knockout littermates (*Mdm2*$^{fl/fl}$*Trp53*$^{+/+}$*alb-cre*) and were not significantly different from those in wild-type littermates (*Mdm2*$^{fl/fl}$*Trp53*$^{+/+}$ *or Mdm2*$^{fl/fl}$*Trp53*$^{fl/fl}$) (Figure 4A). Picrosirius red staining of the liver tissue demonstrated that spontaneous liver fibrosis was completely abolished in the double-knockout mice (Figure 4B) and collagen deposition was significantly lower in the double-knockout mice than in the Mdm2-knockout littermates (Figure 4C). Type I collagen gene expression also significantly decreased in the double-knockout mice compared with the single-knockout mice and was not different from that in wild-type littermates when assessed by real-time RT-PCR (Figure 4D). These findings clearly demonstrated that the spontaneous liver fibrosis in the Mdm2-knockout mice was completely dependent on p53,

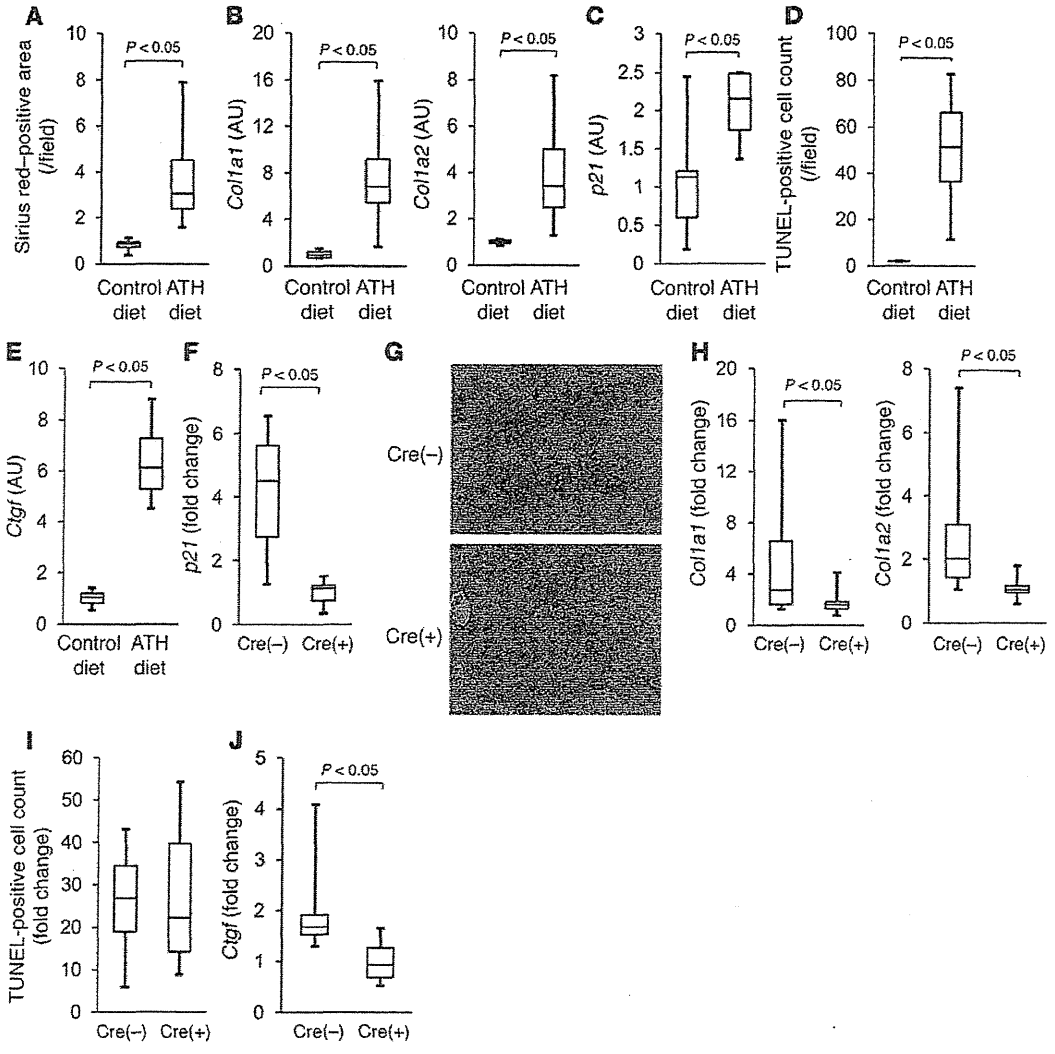

Figure 5

Hepatocyte-specific p53-knockout mice show alleviated liver fibrosis induced by ATH diet with suppression of the CTGF increase. (**A–E**) C57BL6/J mice were fed ATH diet or control diet for 4 weeks and then examined; 4 mice per group. (**A**) Liver fibrosis was evaluated by picrosirius red staining of liver sections. (**B**) *Col1a1* and *Col1a2* mRNA levels in the liver were determined by real-time RT-PCR. (**C**) *p21* mRNA levels in the liver were determined by real-time RT-PCR. (**D**) Hepatocyte apoptosis was evaluated by TUNEL staining of liver sections. (**E**) *Ctgf* mRNA levels in the liver were determined by real-time RT-PCR. (**F–J**) *Trp53*$^{fl/fl}$ [(Cre(–)] mice and *Trp53*$^{fl/fl}$*alb-cre* [Cre(+)] mice were fed ATH diet or control diet for 4 weeks and then examined; more than 6 mice per group; data are presented as fold change in the ATH diet group compared with the control diet group. (**F**) *p21* mRNA levels in the liver were determined by real-time RT-PCR. (**G**) Liver fibrosis was evaluated by picrosirius red staining of the liver sections. Original magnification, ×100. (**H**) *Col1a1* and *Col1a2* mRNA levels in the liver were determined by real-time RT-PCR. (**I**) Hepatocyte apoptosis was evaluated by TUNEL staining of liver sections. (**J**) *Ctgf* mRNA levels in the liver were determined by real-time RT-PCR.

indicating that endogenous p53 activation in hepatocytes causes spontaneous liver fibrosis. ALT levels were normalized in the double-knockout mice, with a significant decrease in TUNEL-positive cells in the liver (Figure 4, E and F). *Ctgf* gene expression was also significantly lower in the double-knockout mice than in the single-knockout mice and was not different from that in wild-type littermates (Figure 4G). These results indicated that hepatocyte p53 activation induced hepatocyte apoptosis and CTGF upregulation in the liver.

Hepatocyte-specific p53-knockout mice show alleviated liver fibrosis induced by ATH diet with suppression of CTGF increase. To investigate the involvement of p53 in liver fibrosis, we examined p53 activation in liver of wild-type mice fed an ATH diet, an experimental model of murine liver fibrosis (24, 25). After 4 weeks of ATH diet feeding, wild-type mice developed liver fibrosis as assessed by hepatic collagen deposition of picrosirius red staining, with upregulation of *Col1a1* and *Col1a2* gene expression (Figure 5, A and B). Regarding the p53-regulated genes, real-time RT-PCR analysis revealed that, in liver of the ATH diet–fed mice, *p21* gene expression levels rose and were significantly higher than those in liver of control diet–fed mice (Figure 5C). This finding suggested that p53 activation had occurred in the liver fibrosis induced by the ATH diet. TUNEL staining of the liver sections showed that hepatocyte

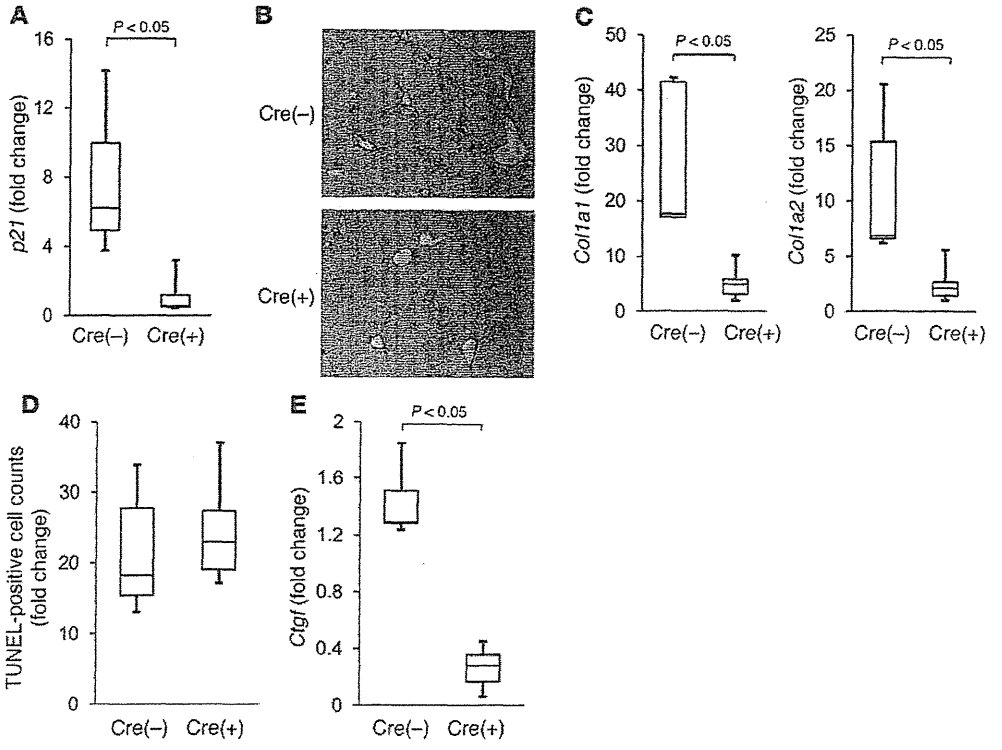

Figure 6

Hepatocyte-specific p53-knockout mice show alleviated liver fibrosis induced by TAA administration, with suppression of the CTGF increase. (**A**–**E**) *Trp53*$^{fl/fl}$ [Cre(–)] mice and *Trp53*$^{fl/fl}$*alb-cre* [Cre(+)] mice were given intraperitoneal injection of 200 mg/kg TAA 3 times per week for 6 weeks and then analyzed; 6 mice per group; data are presented as fold change in the TAA-treated group compared with the nontreated group. (**A**) *p21* mRNA levels in the liver were determined by real-time RT-PCR. Original magnification, ×100. (**B**) Liver fibrosis was evaluated by picrosirius red staining of the liver sections. (**C**) *Col1a1* and *Col1a2* mRNA levels in the liver were determined by real-time RT-PCR. (**D**) Hepatocyte apoptosis was evaluated by TUNEL staining of liver sections. (**E**) *Ctgf* mRNA levels in the liver were determined by real-time RT-PCR.

apoptosis significantly increased in ATH diet–fed mice compared with the control diet–fed mice (Figure 5D). Moreover, with this ATH diet, *Ctgf* gene expression significantly increased in the liver (Figure 5E). To investigate whether p53 activation was involved in the progression of liver fibrosis provoked by the ATH diet, the hepatocyte-specific p53-knockout mice (*Trp53*$^{fl/fl}$*alb-cre*) and the control littermates (*Trp53*$^{fl/fl}$) were fed the ATH diet or control diet, and then liver fibrosis was examined. After 4 weeks of feeding on the ATH diet, the *p21* gene was upregulated in the control littermates but not in the knockout mice, thus confirming p53 activation in hepatocytes in this fibrosis model (Figure 5F). Picrosirius red staining of the liver tissues revealed that liver fibrosis was alleviated in the knockout mice compared with the control littermates (Figure 5G). Real-time RT-PCR study demonstrated that the ATH diet–induced increase in *Col1a1* and *Col1a2* gene expression was significantly attenuated in the knockout mice compared with control littermates (Figure 5H). These results indicated that inhibition of p53 activation in hepatocytes alleviated the liver fibrosis caused by the ATH diet. With this ATH diet, hepatocyte apoptosis increased similarly in both groups compared with the control diet, and there was no significant difference between them in the increase, when assessed by TUNEL staining of the liver tissue (Figure 5I). This finding suggested that p53-dependent hepatocyte apoptosis was not much involved in this model. On the other hand, while the ATH diet upregulated *Ctgf* gene expression in the control littermates, this did not occur in the knockout mice (Figure 5J), suggesting that p53-mediated CTGF upregulation may be involved in the progression of liver fibrosis caused by the ATH diet.

Hepatocyte-specific p53-knockout mice show alleviated liver fibrosis induced by thioacetamide administration, with suppression of the increase in CTGF. To further investigate the involvement of p53 in another well-established model of liver fibrosis, we used repetitive intraperitoneal injection of thioacetamide (TAA) (26) to examine the hepatocyte-specific p53-knockout mice and control littermates. Upon 6 weeks of TAA administration, *p21* gene expression increased in the control littermates but not in the knockout mice, and there was a significant difference between them in its upregulation (Figure 6A). These findings suggested that p53 activation occurred in this fibrosis model as well. Picrosirius red staining of the liver sections revealed that liver fibrosis was alleviated in the knockout mice compared with control littermates (Figure 6B). Real-time RT-PCR study demonstrated that TAA-induced increases in *Col1a1* and *Col1a2* gene expression were significantly attenuated in the knockout mice compared with control littermates (Figure 6C). These results indicated that inhibition of p53 activation in hepatocytes alleviated TAA-induced liver fibrosis. TAA treatment increased hepatocyte apoptosis in both groups to a similar extent, as assessed by TUNEL staining of the liver tissue (Figure 6D). On the other hand, upon TAA treatment, there was a significant difference between them in the CTGF increase

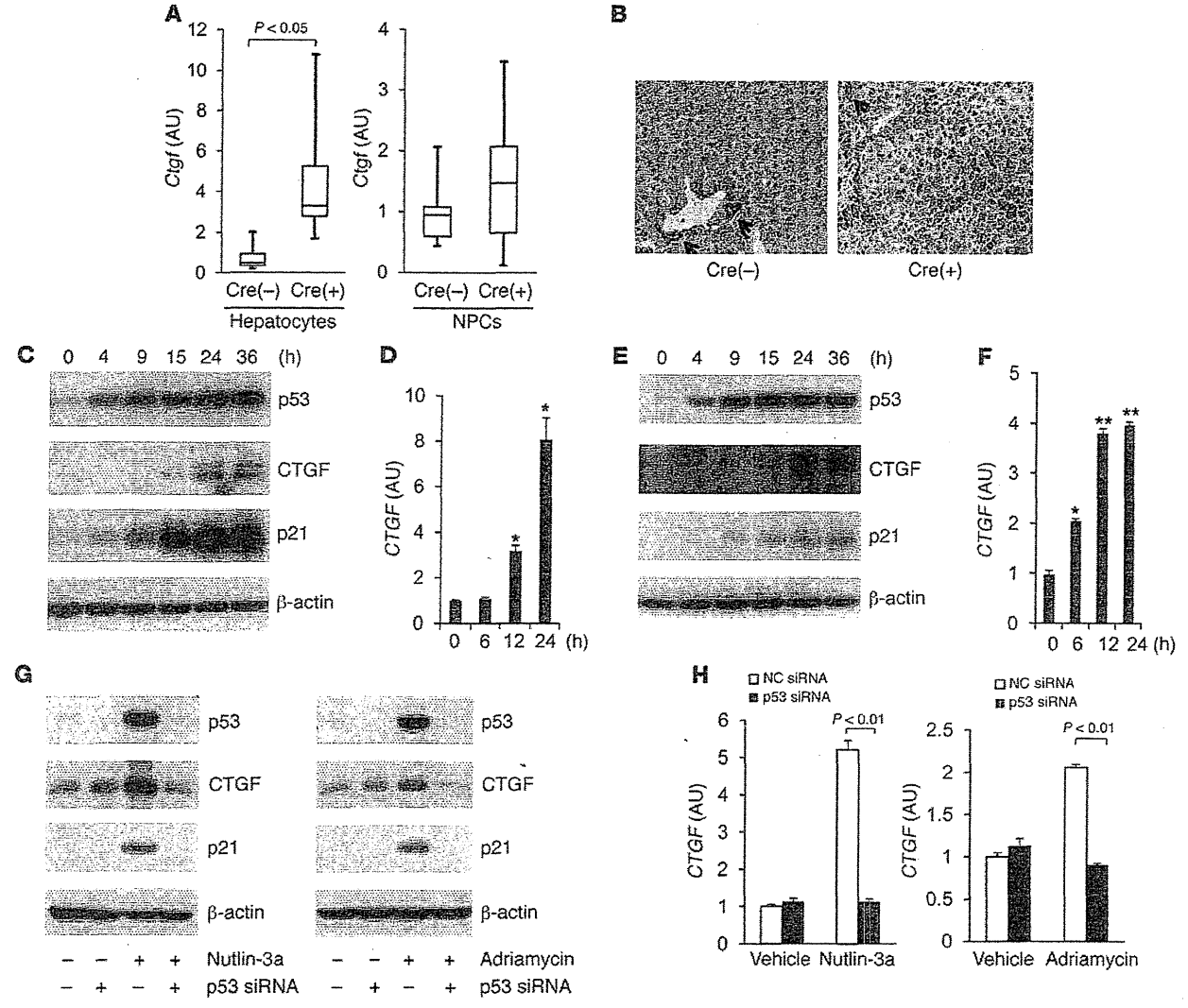

Figure 7

p53 regulates CTGF synthesis in hepatocytes. (**A**) Hepatocytes and NPCs were isolated from *Mdm2*$^{fl/fl}$ [Cre(–)] mice and *Mdm2*$^{fl/fl}$*alb-cre* [Cre(+)] mice by collagenase-pronase perfusion of the liver. *Ctgf* mRNA levels in the isolated hepatocytes (left panel) and NPCs (right panel) were determined by real-time RT-PCR; 4–6 mice per group. (**B**) Expression of CTGF protein in liver sections was assessed by immunohistochemistry; black arrows indicate cholangiocytes. Original magnification, ×200. (**C** and **D**) HepG2 cells (1.0×10^5) were treated with nutlin-3a (20 μM) or vehicle for the indicated time courses. (**C**) Western blot analysis of p53, CTGF, and p21 proteins. (**D**) Real-time RT-PCR analysis of *CTGF* mRNA expression; $n = 3$/group; $^*P < 0.01$ versus the other 3 groups. (**E** and **F**) HepG2 cells (1.0×10^5) were treated with Adriamycin (1 μM) or vehicle for indicated time courses. (**E**) Western blot analysis of p53, CTGF, and p21 proteins. (**F**) Real-time RT-PCR analysis of *CTGF* expression; $n = 3$/group; $^*P < 0.01$ versus the other 3 groups, $^{**}P < 0.01$ versus 0- and 6-hour groups. (**G** and **H**) HepG2 cells were transfected with *p53* siRNA or control siRNA for 3 days and then cultured for 24 hours with nutlin-3a (20 μM), Adriamycin (1 μM), or vehicle. (**G**) Western blot analysis of p53, CTGF and p21 proteins. (**H**) Real-time RT-PCR analysis of *CTGF* mRNA expression; $n = 3$/group, statistical analyses were performed by the paired *t* test.

(Figure 6E). These findings suggested that p53-mediated CTGF upregulation may be also involved in the progression of liver fibrosis provoked by TAA treatment.

p53 regulates CTGF synthesis in hepatocytes. We tried to identify the cells in which CTGF synthesis increased in the liver of hepatocyte-specific Mdm2-knockout mice. *Ctgf* gene expression in the hepatocytes of the knockout mice was significantly higher than in the control littermates (Figure 7A), while it did not significantly differ between them in the non-parenchymal cells (NPCs) (Figure 7A). Immunohistochemical examinations in the liver sections also revealed that CTGF was expressed in hepatocytes of the knockout mice, but not in those of control littermates (Figure 7B). On the other hand, CTGF was expressed in cholangiocytes of both groups of mice, but its levels were not much different between them. These findings suggested that p53 activation induced CTGF synthesis in murine hepatocytes. Next, to investigate the involvement of p53 in CTGF regulation in human hepatocytes, we performed an in vitro study using HepG2 cells, which are known to preserve wild-type p53 function (27). Administration of nutlin-3a into HepG2 cells led to time-dependent increases in p53 and p53-regulated gene

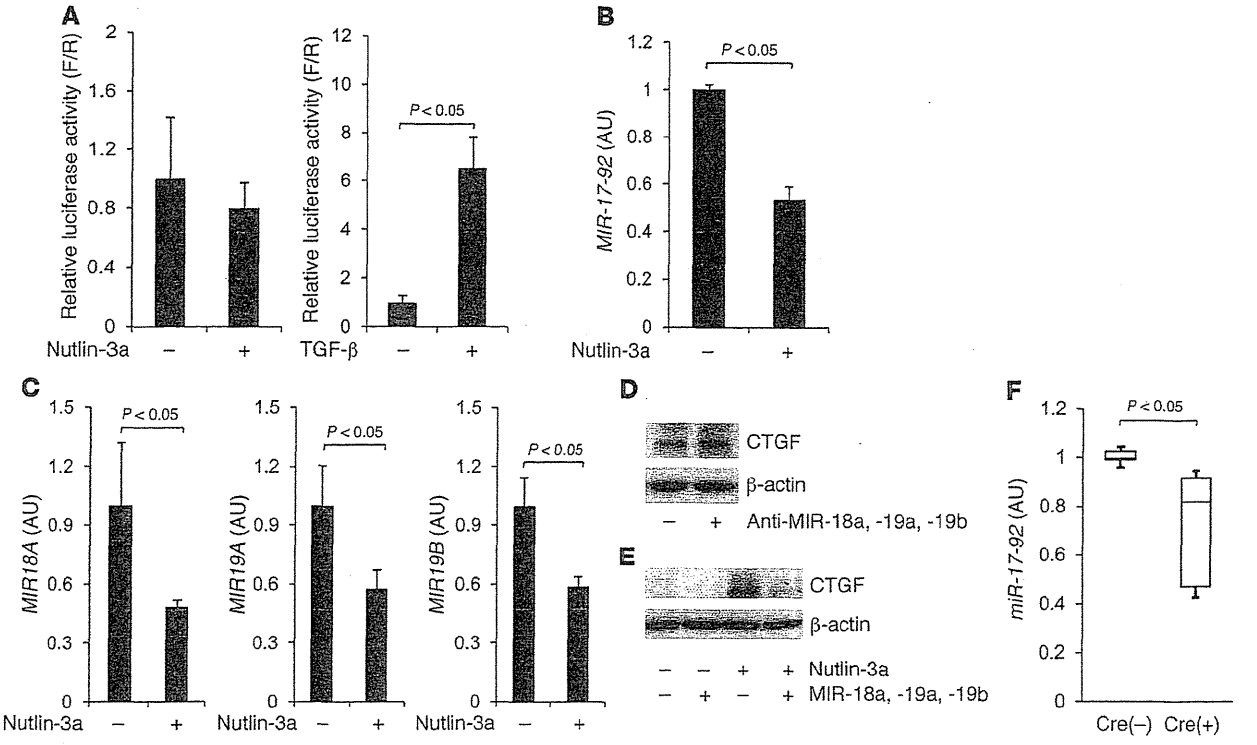

Figure 8

p53 activation upregulates CTGF synthesis via repression of the *miR-17-92* cluster gene. (**A**) HepG2 cells (1.0×10^5) were cotransfected with pTS-589 and pRL-TK for 48 hours and treated with nutlin-3a (20 μM) or recombinant TGF-β (10 ng/ml) for 24 hours. Firefly luciferase and *Renilla* luciferase activity was measured and is presented as relative luminescence values for firefly luciferase versus *Renilla* luciferase (F/R). $n = 4$/group. (**B** and **C**) HepG2 cells (1.0×10^5) were treated with nutlin-3a (20 μM) or vehicle for 24 hours. (**C**) Real-time RT-PCR analysis of *miR-17-92* mRNA (**B**), *MIR18A*, *MIR19A*, and *MIR19B* miRNA expression; $n = 3$/group. Statistical analyses were performed by the paired *t* test (**A–C**). (**D**) HepG2 cells were transfected with a mixture of antisense of *MIR18A*, *MIR19A*, and *MIR19B* at 100 nM each or negative control at 300 nM for 2 days. Expression of CTGF protein was assessed by Western blotting. (**E**) HepG2 cells were transfected with a mixture of precursor of *MIR18A*, *MIR19A*, and *MIR19B* at 10 nM each or negative control at 30 nM for 2 days and cultured with nutlin-3a (20 μM) or vehicle for 24 hours. Expression of CTGF protein was assessed by Western blotting. (**F**) Expression of *miR-17-92* mRNA in isolated hepatocytes was assessed by real-time RT-PCR. Cre(+), *Mdm2*$^{fl/fl}$*alb-cre*; cre(–), *Mdm2*$^{fl/fl}$; 5 mice per group.

products, represented by p21 (Figure 7C), indicating that nutlin-3a could activate p53 in these cells. Upon nutlin-3a treatment, *CTGF* gene expression increased in a time-dependent manner in HepG2 cells (Figure 7D), while *TGFB1* and *PDGFB* gene expression did not (Supplemental Figure 7). We also observed that CTGF protein levels gradually increased upon nutlin-3a treatment (Figure 7C). Adriamycin, a DNA-alkylating agent, could also activate p53, leading to upregulation of CTGF mRNA and protein levels in HepG2 cells in a time-dependent manner (Figure 7, E and F). Administration of *p53* siRNA into HepG2 cells efficiently reduced p53 expression, which was demonstrated by the mRNA levels (Supplemental Figure 8) and protein levels (Figure 7G), and inhibited upregulation of p21 protein upon treatment with nutlin-3a and Adriamycin (Figure 7G). Under this condition, p53 knockdown completely abolished the increase in CTGF that had resulted from administration of these drugs (Figure 7, G and H). These results clearly demonstrated that the increase in CTGF synthesis by nutlin-3a or Adriamycin was completely dependent on p53 in HepG2 cells, indicating that p53 positively regulates CTGF synthesis in human hepatocytes. To directly demonstrate the effect of p53 on CTGF expression in vivo, we injected a p53 expression plasmid, ORF9-mp53, or its control plasmid into BALB/c mice via the tail vein by a hydrodynamic injection procedure (28) and examined *Ctgf* gene expression 2 days later. Although hydrodynamic injection of the p53 expression plasmid only led to nuclear expression of p53 in hepatocytes at a rate of approximately 5% (Supplemental Figure 9A), it significantly increased *Ctgf* gene expression in the liver compared with the control hydrodynamic injection (Supplemental Figure 9B). These results also demonstrated the existence of the p53/CTGF pathway in vivo.

p53 activation upregulates CTGF synthesis via repression of the miR-17-92 cluster gene. Next, we tried to elucidate the molecular mechanism underlying CTGF regulation by p53 in HepG2 cells. To examine whether p53 transcriptionally upregulates *CTGF* gene expression, we introduced plasmid pTS-589 – which contains the *CTGF* promoter from 802 base pairs upstream of the transcript start site to 22 base pairs downstream of the coding sequence linked to the upstream of a firefly luciferase reporter gene (29) – into HepG2 cells. Then, we evaluated the transcription activity of the *CTGF* promoter upon treatment with nutlin-3a or recombinant TGF-β, which is known to transcriptionally upregulate CTGF (29). Whereas luciferase activity increased upon TGF-β treatment, it did not